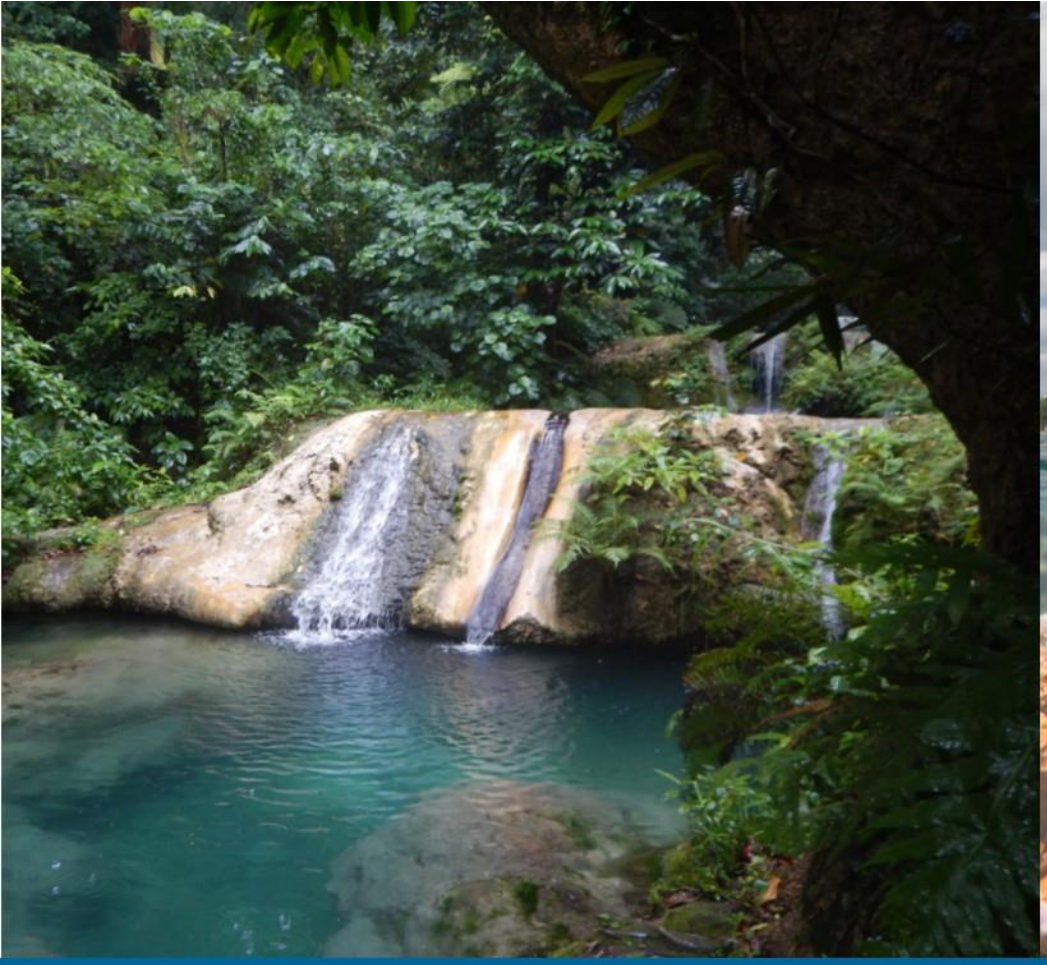

Identification of priority sites for future upscaling of R2R investments, Vanuatu

Prepared for Ridge-to-reef Programme,
GeoScience, Energy & Maritime Division,
SPC

by Seascape Solutions, LLC

December 2019

Identification of priority sites for future upscaling ridge-to-reef investments in Vanuatu

Prepared by:
Seascape Solutions LLC

December 2019

Published by: SPC, Suva, Fiji

Citation: Delevaux, J.M.S. & Stamoulis, K.A. (2019) Identification of priority sites for future upscaling ridge-to-reef investments in Vanuatu. Suva, Fiji SPC, 48 pp

Layout by: SPC

TABLE OF CONTENTS

ABBREVIATIONS

- DEM Digital Elevation Model
- GEBCO General Bathymetric Chart of Oceans
- GEM Geoscience, Energy and Maritime
- GIS Geographic Information System
- HYCOM Hybrid Coordinate Ocean Model
- InVEST Integrated Valuation of Ecosystem Services and Tradeoffs
- LULC Land Use and Land Cover
- MPA Marine Protected Area
- R2R Ridge to Reef
- RUSLE Revised Universal Soil Loss Equation
- SDR Sediment Delivery Ratio
- SPC Pacific Community
- SST Sea surface temperature.
- TPA Terrestrial Protected Area
- TSS Total Suspended Sediment

LIST OF FIGURES

LIST OF TABLES

EXECUTIVE SUMMARY

Island conservation is critical to global conservation because islands represent hotspots of unique biological and geophysical diversity. Islands are also hotspots of biocultural diversity, where natural resources sustain the livelihoods of over 40 million people and help shape cultural identity and wellbeing. Today both biodiversity and human wellbeing on islands are at risk due to growing populations, overexploitation of natural resources, and climate change impacts on both the land and sea, among other factors. Given limited resources for conservation, accessible, easy-to-use conservation planning tools that are appropriate for island contexts are critically needed, especially those that incorporate ridge-to-reef connections and consider human wellbeing.

We adapted and implemented a fine-scale spatially explicit (~30 x 30 m) decision support framework in Vanuatu to support regional resource managers. The tool used existing and global open access geospatial datasets and literature to identify where terrestrial conservation initiatives may have the greatest impact on marine conservation in Vanuatu. Coupled with scenario planning, we identified priority land areas for forest conservation that can maximize downstream benefits.

The key outcomes are as follows: -

(i) Identification of coral reef areas that can be vulnerable to sediment runoff in Vanuatu;
(ii) Identification of priority forest conservation areas on the land that can have the greatest impact on marine conservation in Vanuatu; and
(iii) The development of a decision support tool to identify synergies and trade-offs in habitat conservation across terrestrial and marine ecosystems at an archipelago scale that can also be applied elsewhere.

Priority watersheds were identified on nearly all the islands modeled. Several island regions are notable in terms of the number of priority watersheds that could potentially impact coral reefs though sedimentation. These included the northeast part of Santo Island, northern Gaua, north Pentecost, west Epi, and north Efate. Tagabe watershed on Efate Island was also selected as a priority. Among the modeled islands, Ambae and Ambrym had the least number of priority watersheds. Areas within each priority watershed which contributed the most to sedimentation and impact downstream coral reefs were also identified. This information should be combined with existing land use plans to further prioritize areas for management actions. The next steps would be to build a suite of land-use management scenarios within the priority areas identified in this study. Then, evaluate tradeoffs to identify optimal management solutions. By adopting a ridge-to-reef conservation planning process, protected areas can be designed for multiple benefits that include improvements in biodiversity, drinking water, and reef fisheries.

This research and modelling work explores the ridge-to-reef concept that integrates natural and human systems, and land and ocean realms, to improve our understanding of island systems and support conservation planning in Vanuatu. The results of this trial can guide the development of a regional guideline for the implementation of the R2R spatial prioritization procedures, and specific case studies in its application in Vanuatu and other Pacific Islands.

1. INTRODUCTION

Islands represent hotspots of unique biological and geophysical diversity and are thus critical to global conservation efforts. Because the high productivity of marine ecosystems is largely confined to coastal areas, islands have an ecological influence on oceans that is disproportionally higher than suggested by their land area (Barnett 2011). Many island societies are highly dependent on local resources, with terrestrial and marine ecosystems influencing the livelihoods of the more than 40 million people and help shape cultural identity and wellbeing (Kueffer and Kinney 2017). Nowadays, many islands support growing populations, which has led to increased pressure on forests and fisheries while natural disasters and climate change exacerbate the pressure on those natural resources (Walker and Bellingham 2011). These impacts affect islanders in a number of ways, such as reducing food resources upon which many islanders depend on for wellbeing (Eriksson et al. 2017).

Global climate change poses increasing threats to both terrestrial and marine ecosystems, where increases in storm frequency and intensity impact ecosystems on land and rising sea temperatures and ocean acidification impact marine ecosystems through bleaching and lowered calcification rates (Hoegh-Guldberg 1999, Anthony 2016). Across much of the tropics, local scale anthropogenic activities, in particular logging and commercial agriculture expansion, are threatening coral reefs through increased sediment and nutrient runoff (Dauvergne 1998, Mather et al. 1998). Excess nutrients and sediments have been shown to impact coral reefs by promoting benthic algae growth and smothering corals, respectively (Fabricius 2005b, Houk et al. 2014, Smith et al. 2016b). Nutrients are known to bind and travel with sediment, thereby potentially contributing to lack of recovery from bleaching through promoting algae growth (Wooldridge 2009a, Wooldridge and Done 2009). For these reasons, integrating land and sea into conservation planning on islands is critical.

The conservation planning tools needed on islands require the recognition of land-sea connections (Klein et al. 2012, Brown et al. 2017b). Due to their small size and often volcanic geology, land and sea are tightly linked through social and ecological processes (Jupiter et al. 2017). Historically, terrestrial and marine ecosystems have been managed and protected in isolation, where terrestrial protected areas (TPAs) and marine protected areas (MPAs) are often designed regardless of downstream or upstream activities (Margules & Pressey 2000, Alvarez-Romero et al. 2011). TPAs can promote downstream benefits when accounting for land and sea connections (Halpern et al. 2008a, Klein et al. 2012, Grorud-Colvert et al. 2014), while MPAs may not be as effective when exposed to high land-based source pollution because conditions upstream are not considered (Bellwood et al. 2004, Halpern et al. 2013b). Therefore, to maximize biodiversity benefits, conservation planning for land and sea should be integrated (Klein et al. 2014).

1.1 PURPOSE & RATIONALE

The goal of this consultancy was to develop a spatial planning procedure that supports an objective approach to site selection for ridge-to-reef (R2R) interventions and reforms. This cost-effective rapid assessment procedure provides the foundation for selecting target sites to begin participatory planning processes in order to upscale future R2R investments in Pacific islands settings. This project built on a fine-scale, spatially explicit decision support framework, previously developed for quantifying the effect of nutrient enriched groundwater and sediment stream runoff on coral reefs in Fiji and Hawai‘i. Here, we adapted, applied, and scaled up this tool to inform conservation actions at the sub-watershed scale across the entire archipelago of Vanuatu. To spatially prioritize terrestrial conservation efforts across the country of Vanuatu based on downstream coral reef impacts, we modeled the potential impacts of projected land-use change on nearshore ecosystems through sediment runoff and traced those back to the areas driving these impacts within each watershed.

The adapted decision support tool for Vanuatu links the Integrated Valuation of Ecosystem Services and Tradeoffs (InVEST) Sediment Delivery Ratio (SDR hereafter) to a water quality model. We leveraged existing global and local datasets from the region to calibrate this linked land-sea decision support tool and identified where terrestrial conservation may provide the greatest benefits for marine conservation. Although nutrients are associated with sediment runoff and agriculture expansion, we did not explicitly model nutrient runoff because of the lack of spatial information on local fertilizer application rates. First, we modeled the sediment export to the shoreline under current and projected land use/cover change and diffused those loads into the marine environment to map Total Suspended Sediment (TSS). Then, we undertook a spatial analysis to identify coral reef areas exposed to a significant change in TSS and we linked those areas to the watersheds driving the changes in water quality. Lastly, we identified priority areas in specific watersheds where implementing conservation actions could reduce sediment runoff and foster coral reef resilience.

2. METHODS

2.1 R2R PROCEDURE OVERVIEW

The procedure for prioritizing and upscaling R2R investments consists of three key components: (1) InVEST SDR, (2) a water quality model, and (3) a spatial impact analysis linking coral reef habitats to watersheds through sediment. Using InVEST SDR, sediment export ($t.yr^{-1}$) was modeled based on current and future land use/cover scenarios, topography, soil types, and rainfall data at 30 m x 30 m resolution for each watershed (Fig 1c-d). The modeled sediment export was diffused from pourpoints representing stream mouths into the marine zone using a water quality model to generate maps of TSS ($t.yr^{-1}$), under present and future land use/cover at 100 m x 100 m (Fig 1e). Using an overlay analysis, we quantified the coral reef areas exposed to sediment runoff under present conditions (Fig 1f-g). Once parameterized for present conditions, we applied this decision-support tool on projected land use/cover change scenarios to identify marine areas exposed to a significant change in sediment runoff and traced those back to identify priority areas within the watersheds where conservation action can promote coral reef resilience (Fig 1i).

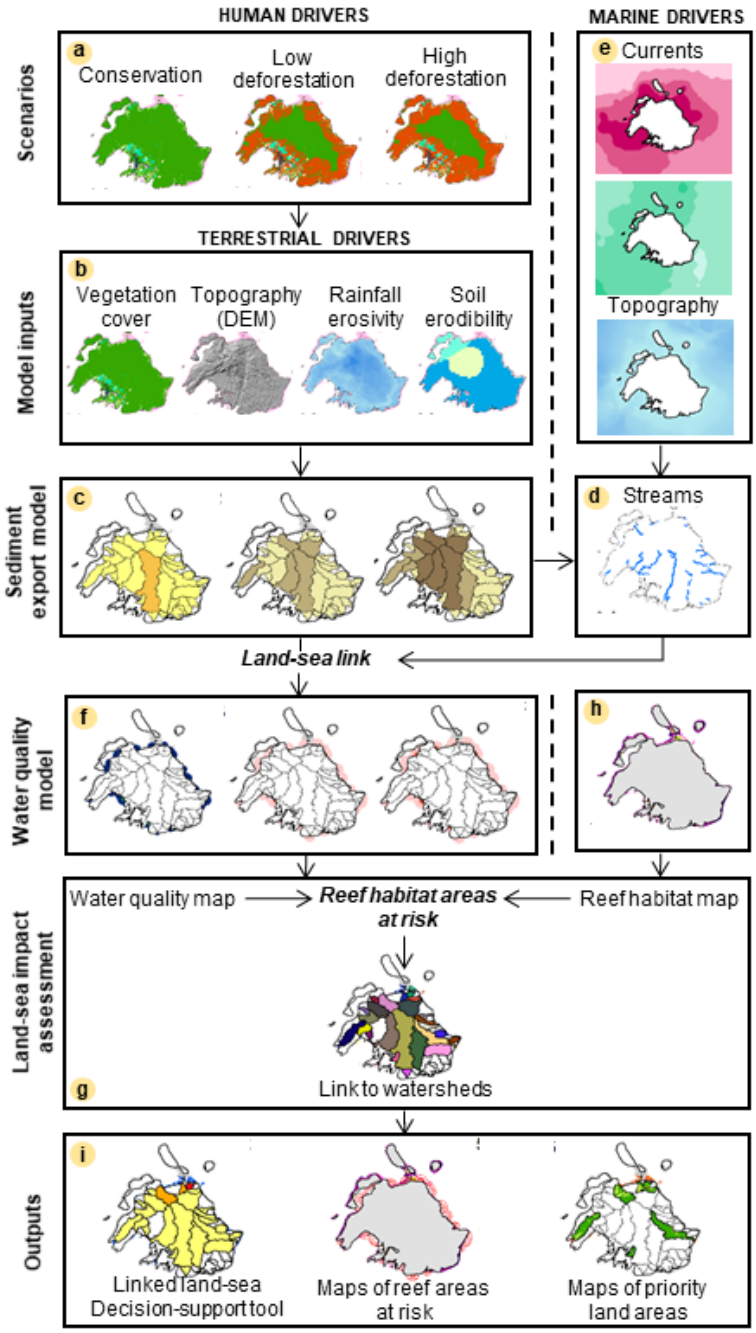

Fig 1. Ridge-to-reef modeling framework. (a) Land-use change scenarios were coupled with the linked land-sea decision support tool; (b) Land cover, topography, rainfall, and soil erodibility data were inputs in (c) InVEST Sediment Delivery Ratio (SDR) model to quantify sediment export (t. yr^{-1}) and assigned to (d) pourpoints at the shoreline and combined with (e) bathymetry and current maps into (f) a water quality model to generate: (g) total suspended sediment (TSS) maps (t. yr^{-1}), which are overlaid with (h) reef habitat maps to (i) identify the priority conservation areas in watersheds linked to reef habitats through sediment. The outputs were: (1) a linked land-sea decision-support tool, (2) maps of reef areas at risk, and (3) maps of priority land areas for conservation.

2.2 SITE DESCRIPTION

The modeled land area represents 17 main islands and a total area 11,663 km^2 (Fig 2). Topographically, Vanuatu's elevation ranges from 0 to 2,769 m and averages 280 m (Fig S1.1-13). The watershed size ranges from 4.6 km^2 to 461.9 km^2, and averages 15.2 km^2. Yearly rainfall varies between 146.3-415.5 mm/yr and averages 244.9 mm/yr (Fig S1.14-26). Based on a global database (Batjes 2016), there are 11 types of soils across the modeled islands (Fig S1.40-53). Downstream, the coral reef habitat area spread across a total of 580 km^2 of mostly narrow reef systems (Fig S2), which drop off quickly into deep water (Fig S3.1). The main currents flow from south to north and east to west (Fig S3.2-3). The coastline stretches across 4,218 km (Fig 2).

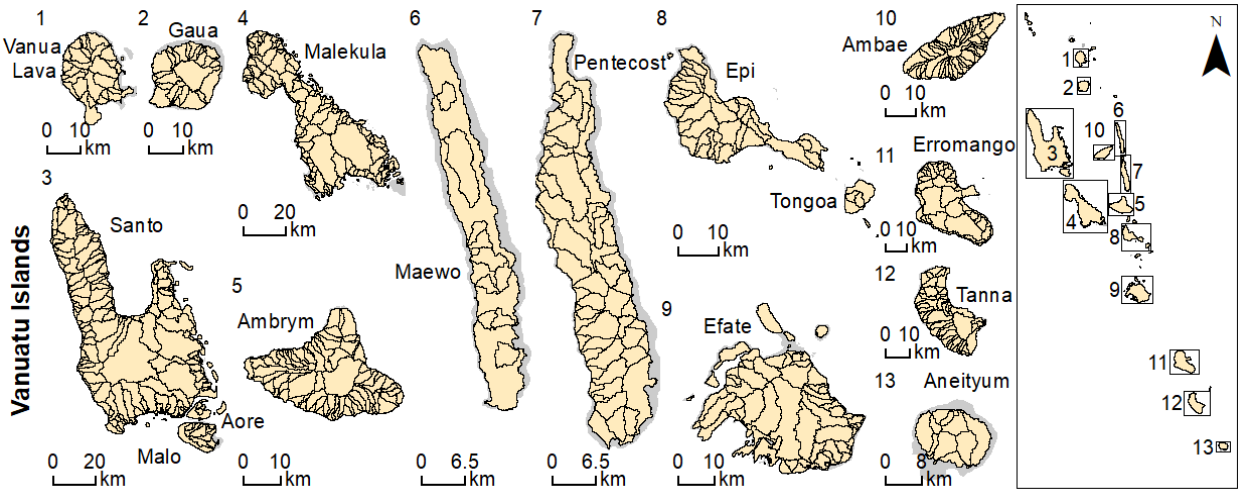

Fig 2. Study site. (1-13) The largest 17 islands of Vanuatu were modeled. Teguna is the smallest modeled island with one watershed and is not provided as an inset.

2.3 SCENARIO DESIGN

Deforestation in Vanuatu occurs primarily through human settlement and agriculture expansion (Eckardt et al. 2008). After the collapse of sandalwood due to overexploitation, the subsequent commercial use of forest ecosystems expanded with the logging and sawing of trees for timber (Regenvanu et al. 1997). Large-scale clearance of forests for the establishment of pastures and coconut plantations had already occurred following land alienation, while the logging industry uses timber from land still held by the traditional owners (Regenvanu et al. 1997). Approximately 80% of all deforestation took place in low elevation terrain (<300 m) (Eckardt et al. 2008). The logging practices code of Vanuatu states that no deforestation should take place on slopes steeper than 30° (McIntosh 2013). About 90 % of the detected deforestations are located within a perimeter of 3,000 meters around settlements (Eckardt et al. 2008). As expected, the biggest fraction of the degraded areas is located in proximity to roads (Eckardt et al. 2008). Hence, both scenarios assumed that deforestation can take place up to 3,000 m around existing human land use and roads.

It was assumed that forest gets converted to human land use (e.g., banana plantation, rice fields, cultivated land, unknown crop, settlement). The low deforestation scenario models human land use expansion (e.g., urban growth, agricultural expansion) in forested land cover on slopes primarily less than 10° and below 300 m elevation, while the high deforestation scenario assumed human land use expansion on slopes primarily less than 20° and below 400m elevation. The logging practices code of Vanuatu states that a 30 m buffer on class 1 streams (> 20 m width), a 20 m buffer on class 2 streams (< 10-20 m width), and a 100 m buffer are applied around lakes, lagoons and the coast. Furthermore, buffer zone widths are doubled where slopes exceed 10 degrees (17%) (McIntosh 2013). To respect the existing logging practices code of Vanuatu, under both scenarios, existing forest habitat in the coastal zone, along streams and rivers were protected by a 100 m, 20 m, and 30 m buffers, respectively. It is important to note that these scenarios are not meant to predict future land uses in any way, nor do they provide any recommendations for sustainable development, but are rather used to illustrate the utility of the soil erosion model and reveal how land use changes affect soil erosion in different regions.

2.4 SEDIMENT MODEL - INVEST SDR

Erosion and overland sediment retention are natural processes that govern the sediment concentration in streams and nearshore regions. Sediment dynamics at the catchment scale are mainly determined by climate (in particular rain intensity), soil properties, topography, and vegetation; and anthropogenic factors such as agricultural activities or dam construction and operation (Sharp et al. 2016). We leveraged the open source InVEST toolbox from the Natural Capital Project for this study. The spatially-explicit SDR model (version 3.2) uses soil erosion equations to identify the land areas supplying sediment loads to stream mouths (Hamel et al. 2015). We applied the InVEST SDR model to quantify the sediment export ($t.yr^{-1}$) to the coast by watershed due to soil loss on hillslopes from overland erosion (Fig 1) (Hamel et al. 2015). SDR is spatially explicit and operates at the resolution of the digital elevation model (DEM) input (30.7 m). For each pixel, the model first computes the amount of sediment eroded from that pixel using the Revised Universal Soil Loss Equation (RUSLE), then computes the sediment delivery ratio (SDR), to estimate the proportion of soil eroded on a given area that will travel to the stream mouth at the shoreline (see Hamel et al. 2015 for full details on the model). This approach relies on modeling sediment transport throughout the landscape based on local topography, and therefore does not require hydrological modeling to determine the sediment ratio exported to the shoreline. This approach was initially proposed by Borselli et al. 2008) and has received increasing interest in recent years (Cavalli et al. 2013, López-Vicente et al. 2013).

First, we estimated the overland gross erosion per cell using the empirical RUSLE (equation 1) (Renard et al. 1997):

$$Soil\ loss = R\ x\ K\ x\ LS\ x\ C\ x\ P \qquad (1)$$

Where R = rainfall erosivity ($MJ.mm.ha^{-1}.hr^{-1}$), K = the rate of soil loss per rainfall erosion index unit, known as soil erodibility ($ton\text{-}ha\text{-}hrs.MJ^{-1}.ha^{-1}.mm^{-1}$), LS = slope-length and gradient factor

(derived from the DEM), C = a vegetation cover (C-factor) and P=management practice effectiveness (P-factor).

The SDR model is based on the concept of hydrological connectivity to estimate sediment retention and export to the shoreline (see Borselli et al. 2008 for more details). First, the SDR computes a connectivity index (IC_i) for each pixel *i* based on the upslope area and downslope flow path (Borselli et al. 2008). A streamflow accumulation threshold was set to define streams based on the DEM (Hamel et al. 2015). Given the lack of empirical data for the region, the connectivity of the model was verified by comparing predicted stream outputs to available stream maps. Then, a sediment delivery ratio is derived for each pixel *i* based on the connectivity index (Hamel et al. 2015). The SDR model parameters include an IC_0, a Borselli k-factor, and a maximum allowable SDR that define the shape of the relationship between the SDR and the connectivity index (Hamel et al. 2015). The calibration parameters IC_0 and the k-factor were set to 0.5 and 2.0, respectively, and the maximum allowable SDR was set to 0.8 (Hamel et al. 2015) (*see* Sharp et al. (2016) for more details on effects of parameterization). The sediment export per present and future scenario are reported at the sub-watershed and island scale. This approach was selected since it requires a minimal number of parameters and is spatially explicit. We note that the models have yet to be quantitatively validated against local datasets and were parameterized with values from other regions, which can differ in terms of climate and soil conditions (Gholami et al. 2009).

2.4.1 Watershed delineation

Sub-watersheds were created by processing the DEM raster dataset (~ 30 x 30 m) of Vanuatu, provided by the Pacific Community (SPC) Fiji Geoscience, Energy and Maritime (GEM) Division, with the ArcHydro toolset in ArcGIS and pourpoints at the shoreline were edited for accuracy in comparison to satellite imagery and bathymetry data (DeVantier and Feldman 1993, Falinski 2016, Delevaux et al. 2018). The first step in processing the DEM was to fill all the sinks in the dataset. That is, any areas where water would get trapped had to be elevated to a point where that would no longer occur. This was accomplished using the Fill Sinks tool. The Flow Direction tool determined the flow path along the terrain. Next, the Flow Accumulation tool calculated the number of grid cells that flow into any given cell in the DEM. At this point there was enough information to define streams within our study area. The Stream Definition tool allows you to choose exactly what the threshold of flow accumulation is which defines a stream. A threshold of 1,000 cells was chosen, or an area of 810,000 m^2. Any cells which have a flow accumulation of 1,000 or more would then be considered part of the stream network for our study area. The next step was to use the Stream Segmentation tool; this function creates a grid of stream segments that have a unique identification. From the output of the Stream Segmentation tool we can then define catchments using the Catchment Grid Delineation tool. There is essentially one catchment created for every stream segment. Next, a vector layer for streams was created using the Drainage Line Processing tool. Additionally, a vector layer for catchments was created using the Catchment Polygon Processing tool. Lastly, drainage points for each catchment were created using the

Drainage Point Processing tool. These points represent where tributaries feed into larger streams and eventually where river mouths let out into the ocean. The outputs were shapefiles representing the watersheds such that each watershed contributes to a point of interest where water quality will be analyzed. Finally, the output stream map was compared to hydrographic maps of the archipelago.

2.4.2 Rainfall erosivity index (R)

The rainfall-runoff erosivity factor (R) represents the erosion potential caused by rainfall. The rainfall-runoff erosivity factor is represented by a raster dataset with an erosivity index value for each cell. This variable depends on the intensity and duration of rainfall in the area of interest. It is defined as the long-term average of the product of total rainfall energy and the maximum 30-min intensity (I30) of rainstorms (Wischmeier and Smith 1978, Renard et al. 1997). The greater the intensity and duration of the rainstorm, the higher the erosion potential. Determining I30 requires at least 20 years of pluviograph data.

Because the erosivity index is widely used, in case of its absence, there are methods and equations to help generate a grid using climatic data. [units: $MJ \cdot mm \cdot (ha \cdot h \cdot yr)^{-1}$]. Mean monthly precipitation data (1950-2000) were obtained from WorldClim's 30 arcsecond resolution Bioclim dataset (Fick and Hijmans 2017). The map of rainfall erosivity was derived from monthly rainfall averages at a 1 km x 1 km (P) and converted to erosivity using the Bols method applied in Indonesia (equation 2):

$$R = \frac{2.5\ x\ P^2}{100(0.073P + 0.73)} \qquad (2)$$

2.4.3 Soil erodibility (K)

Soil erodibility (K) is a measure of the susceptibility of soil particles to detachment and transport by rainfall and runoff. [units: $tons \cdot ha \cdot h \cdot (ha \cdot MJ \cdot mm)^{-1}$]. K represents an integrated average annual value of the total soil and soil-profile reaction to many erosion and hydrologic processes. These processes include soil detachment and transport by raindrop impact and surface flow, localized deposition due to topography and tillage-induced roughness, and rainwater infiltration into the soil profile (Renard et al. 1997). It is defined as the rate of soil loss per erosivity index unit as measured on a standard plot 22.1 m long with a 9% slope, and continuously in a clean-tilled fallow condition, with tillage performed upslope and downslope (Renard et al. 1997). When profile permeability and structure are not available, soil erodibility can be estimated based on soil texture and organic matter content, based on the work of Wischmeier, Johnson and Cross (reported in (Roose 1977).

K was derived from the global World Inventory of Soil Emission Potentials (WISE)soil database (Batjes 2016). A special case is the K value for water bodies, for which soil maps may not indicate

any soil type. A value of 0 can be used, assuming that no soil loss occurs in water bodies. We clipped the soil map to Vanuatu and joined the table (Table: HW30s_MapUnit) from the global database to obtain the soil types for the region. The dataset included spatially categorized soil types based on similarities in soil characteristics. Each category contained information on percent organic matter, the product of the primary particle size fraction, and the percent of the top six abundant soil types. For this study, we only focused on the topsoil. So, we only needed to join with the topsoil Table PRID (HW30s_ParEst) from the global database. The K-factor was derived using equation 3 (Williams 1995) and the WISE derived soil properties on a 30 by 30 arc-seconds global grid (Batjes 2016).

$$K = f_{csand} \cdot f_{cl-si} \cdot f_{orgc} \cdot f_{hisand} \quad (3)$$

Where: f_{csand} = a factor that gives low soil erodibility factors for soils with high coarse-sand contents and high values for soils with little sand, expressed in $(\mathrm{ton/ha})^{*}(\mathrm{ha.hr/MJ.mm})$ or $\mathrm{t{\cdot}ha{\cdot}hr{\cdot}(MJ{\cdot}mm{\cdot}ha)^{-1}}$, f_{cl-si} = a factor that gives low soil erodibility factors for soils with high clay to silt ratios, f_{orgc} = a factor that reduce soil erodibility for soils with high organic carbon content, f_{hisand} = a factor that reduces soil erodibility for soils with extremely high sand contents. The soil erodibility values (K) in this table are in US customary units, and require the 0.1317 conversion (FAO 2007). The input factors of equation 3 are calculated with equations 4-7 below (Williams 1995):

$$f_{csand} = 0.2 + 0.3 \cdot exp\,[-0.256 \cdot ms \cdot (1 - m_{silt}/100)] \quad (4)$$

$$f_{cl-si} = m_{silt}/(m_c + m_{silt})^{0.3} \quad (5)$$

$$f_{orgc} = 1 - (0.0256 \cdot \mathrm{orgC}\,/(\mathrm{orgC} + \exp\,[3.72 - 2.95 \cdot \mathrm{orgC}]) \quad (6)$$

$$f_{hisand} = 1 - (0.7 \cdot (1 - ms/100))/((1 - m_s/100) + exp(-5.51 + 22.9 \cdot (1 - m_s/100)) \quad (7)$$

Where: m_s = % sand content, m_{silt} = % silt content, m_c = % clay content, orgC = % organic carbon. Soil erodibility is represented by a raster dataset, with a soil erodibility value for each cell (Fig S1.40-53).

2.4.4 Land use/cover factors

The land use/cover map was a shapefile provided by SPC Fiji GEM and it represents the most current available land use/cover. The Cover Management Factor (C) represents the effect of vegetation on soil erosion rates (Renard et al. 1997). It is the ratio of soil loss of a specific crop to the corresponding soil loss under the condition of continuously fallow and tilled land (Renard et al. 1997). The amount of protective coverage provided by the flora influences the soil erosion rate. Continuously fallowed and bare soils have a C value equal to 1. C values are lower when more vegetative coverage protects soils against erosion. Well-protected soils have a C value near 0. C-factors assigned to each land cover use/type in Vanuatu were derived from existing literature as estimated based on studies conducted in similar regions containing comparable land uses, from

areas with similar geographic and physical processes, and consultation with experts (see Table 1 for more details on parameters) (Roose 1977, Wischmeier and Smith 1978, FAO 2007, Lianes et al. 2009, Doheny et al. 2013, Chicas and Omine 2015). The Conservation Practice Factor (P) represents the impact of a specific conservation practice on soil erosion rates (Renard et al. 1997). It is the ratio of soil loss of a specific practice to the corresponding soil loss caused by up and down slope culture (Renard et al. 1997). Management practice effectiveness (P factor) was not considered in this model due to lack of data (Hamel et al. 2015). Therefore, we assume the P value to be 1 throughout the entire region. Assigning C and P values to corresponding land uses was done by editing the attribute table of the land use shapefile in ArcGIS.

Table 1. C-factors of land use/cover types.

Land use/cover	C-factor	Source
Airstrip	0.3	'Roads' (Rude et al. 2016)
Banana	0.2	(FAO 2007)
Barren land	1	(Roose 1977, El-Swaify et al. 1982, Doheny et al. 2013)
Cassava	0.5	(FAO 2007)
Coconut forest	0.01	Adapted from (FAO 2007)
Coconut Plantation/crops	0.02	(FAO 2007)
Cultivated land	0.24	(Evensen et al. 2001)
Forest	0.006	'Second growth forest with shrubs patches' (FAO 2007)
Grassland	0.014	'Pasto' c-factor, without grazing (FAO 2007, Lianes et al. 2009)
Legumes	0.02	'Cassava with well-established leguminous crops' (FAO 2007)
Limestone	0.75	Derived from (Karydas et al. 2013)
Navel Nut Tree/Noni tree	0.1	'Orchard' and '*Morinda citrifolia*' (a fruit-bearing tree coffee family) (OMAFRA 2019)
New human land-use	0.25	Human settlement and subsistence agriculture (FAO 2007, Doheny et al. 2013)
Pine plantation	0.007	(FAO 2007)
Plantation	0.3	(Doheny et al. 2013),
Rice	0.2	(FAO 2007)
Rock shelves	0.05	Derived from (Karydas et al. 2013)
Sand Bay	0.003	(Falinski 2016)
Settlement	0.25	(FAO 2007, Doheny et al. 2013)
Shrubs	0.013	"Potrero" (Lianes et al. 2009)
Sugarcane	0.51	(Evensen et al. 2001)
Volcanic ash plain	0.03	TBD
Yams	0.5	(FAO 2007)

2.5 WATER QUALITY MODEL

2.5.1 Stream pourpoints

Pourpoints were created along with sub-watersheds boundaries using the DEM (~ 30 x 30 m) of Vanuatu, provided by SPC Fiji GEM, with the ArcHydro toolset in ArcGIS. The pourpoint shapefile layer is the link between the terrestrial and marine models. The attribute table contains the watershed unique ID and the SDR results. The pourpoints at the shoreline were edited for accuracy in comparison to satellite imagery and the available stream map (DeVantier and Feldman 1993, Delevaux et al. 2018). Then the pourpoint shapefile was split into individual shapefiles for each pourpoint using the watershed unique ID. Finally, the pourpoints were manually edited to align with stream discharge and the marine geospatial layers (e.g., bathymetry and currents).

2.5.2 Decay function

To model the impact of sediment runoff on coastal water quality, we generated a water quality map (30 x 30 m) representing the total sediment load (represented by TSS) from all the watersheds discharging into Vanuatu coastal waters, for each land-use scenario. First, the sediment export from each watershed was diffused in coastal waters by adapting a previously developed dispersal plume models in ArcGIS to represent the point source nature of stream discharge in the local coastal water conditions (Halpern et al. 2008b, Delevaux et al. 2018) (Fig 1). To do so, we created a cost-path surface (c) that quantifies the least accumulative cost-distance (impedance) of moving planimetrically through each cell from each pour point using a composite of three marine drivers known to affect sediment dispersion: depth (m), distance to stream mouth (m), and current (degree and seconds) (*see* 'Distance cost raster' section below for more details) (Yu et al. 2003, Fabricius 2005a, Delevaux et al. 2018). Then, the spread of sediment into coastal waters from each pour point was modeled using a decay function, which assigned a portion of the remaining quantity from the previous cell in all adjacent cells, based on the cost-path surface until a maximum distance of 3 km from the shoreline was reached (Halpern et al. 2008b, Delevaux et al. 2018) (equation 8). This threshold was based on the minimum distance between river mouths measured in ArcGIS.

$$S_i = s_p \times e^{-c^2/D_c} \qquad (8)$$

where S_i= Grid cell value for dispersed sediment (t.yr^{-1}) for watershed i, s_p = Sediment (m^3.yr^{-1}) load (t.yr^{-1}) at each watershed pour point (obtained from summarizing the total sediment export per watershed), c = cost-path surface (unitless), D_c = cost-path surface threshold distance from the shore for each decayed sediment plume per watershed (equivalent to 3 km from the shoreline). Last, we summed all the individual watershed sediment plume gridded maps in ArcGIS to obtain the total sediment load (represented by TSS) per land-use scenario for each pixel of coral reef area. This approach to modeling coastal sediment discharge is diffusive, and thus allows for wrap around coastal features, but does not account for nearshore advection that acts to push suspended sediment in specific directions (Halpern et al. 2008b). We used these diffusive models to derive conservative

estimates of sediment plumes, since the nearshore circulation patterns were unknown for our study site.

2.5.3 Diffusion factors

A diffusion factor raster, which accounts for the effect of depth and current forcing on each grid cell, was generated for each watershed in ArcGIS. The total diffusion factor raster layer was generated by summing and the unitless current and depth diffusion factor layers for each watershed in R. The current and depth diffusion factor raster layers were derived from the current (HYCOM) and bathymetry (GEBCO) data using the methods described below:

2.5.3.2 Depth diffusion factor layers

The bathymetry layer used for this study is the General Bathymetric Chart of Oceans (GEBCO) (~500 m x 500 m) and was downloaded from https://www.gebco.net/ for the area of interest (Weatherall et al. 2015). The dataset was converted to a point shapefile and the nearshore gaps were filled using the Inverse Distance Weighting interpolation tool in ArcGIS. The final bathymetry raster dataset used for this analysis was resampled to 100 m x 100 m. In R, the bathymetry layer was reclassified into 20 bins based on quantiles. The output was a unitless depth diffusion factor layer, ranging from 0 to 20, which assumes that sediment settles out more quickly from the water column in deeper waters (Delevaux et al. 2018).

2.5.3.1 Current diffusion factor layers

First, we determine the travel time layer from each pourpoint due to the currents using the HYbrid Coordinate Ocean Model (HYCOM) average monthly surface currents data. To determine how surface currents could affect the lateral movement of sediment we used the path distance tool in ArcGIS (Doheny et al. 2013, Rude et al. 2016). The path distance tool creates an output raster in which each cell is assigned the accumulative cost from the cheapest source cell while accounting for surface distance and horizontal and vertical cost factors. The algorithm utilizes a node/link cell representation. The cost to travel between one node and the next depends on the spatial orientation of the nodes. How the cells are connected impacts the travel cost as well.

This tool requires (1) a source (i.e., the individual river mouth pourpoint shapefiles), (2) cost raster (seconds), (3) input horizontal raster (degree), and (4) a horizontal factor. The horizontal factor is a user-specified parameter required for the path distance tool that defines the relationship between the horizontal cost factor (seconds to cross each cell) and the horizontal relative moving angle (degree). The horizontal factor defines the horizontal difficulty encountered when moving from one cell to the next (ESRI 2011). The horizontal relative moving angle identifies the angle between the horizontal direction of a cell and the moving direction (ESRI 2011).

For the horizontal factor, we had no additional data other than HYCOM average monthly surface currents, therefore we had no information to tell us that sediment would go anywhere other than "downstream." To address this, we chose to use the "forward" pre-set parameter setting which establishes that only forward movement is allowed (i.e., down-current). The result of this model was an accumulated cost, in seconds to travel towards or away from each river mouth in our study region while accounting for surface current forcing.

The input cost raster and the horizontal raster were both derived from our HYCOM surface current data. To determine mean monthly ocean currents around Vanuatu, we used the HYCOM (HYCOM 2013). HYCOM models are isopycnal (constant potential density) in the open, stratified ocean, which is the only regional data that were available to us for this study. The spatial resolution of the data is 1/12° (~9 km). To acquire the HYCOM data we used the get.hycom function from the HMMoce package (Braun et al. 2018), in R to download 10 years of HYCOM surface current data (1993-2002) to overlap with the precipitation data used for the SDR modelling (1950-2000).

In this study, we used the mean yearly east-west (u) and north-south (v) velocity components of the surface currents. R package ncdf4 (Pierce 2019) was used to manipulate the netcdf files and store the extracted data in a three-dimensional array. Arrays were converted to raster bricks and current data were averaged by month and then by year using the raster package in R (Hijmans 2019). Finally, current data was averaged for the entire 10-year period for u and v variables and output as rasters. The datasets were clipped for Vanuatu coastline and converted to a point shapefile in ArcGIS. The nearshore gaps were filled using the Inverse Distance Weighting interpolation tool in ArcGIS and converted to 100 m x 100 m resolution rasters.

We used Raster Calculator to derive the time in seconds that it would take to cross an individual cell. To do this we took the width of each pixel (100 m) and divided it by the resulting velocity of the two interpolated annual monthly averaged u (E-W) and v (N-S) vectors (in m s-1) derived from HYCOM data (1993-2002) (Doheny et al. 2013) (equation 9):

$$Seconds = \frac{Distance\ across\ the\ cell}{\sqrt{(u^2) + (v^2)}} \quad (9)$$

For the horizontal raster, we needed to determine the direction the resulting vector was going across each cell. We did this by taking our u and v velocities and determining an angle of movement. To determine this angle for each pixel we used the following function in Raster Calculator:

$$Degree = (|\,\mathrm{ATan2}(u, v) * \frac{180}{\pi}| - 180) \quad (10)$$

Lastly, we determined the travel time cost from each pourpoint due to the current data. The accumulated cost, in seconds to travel towards or away from each river mouth in our study region while accounting for surface current forcing, was reclassified into 20 bins based on quantiles. The

output was a current diffusion factor layer, which assumed that the diffusion factor increases with distance from the stream mouth (Delevaux et al. 2018).

2.6 RIDGE-TO-REEF IMPACT ASSESSMENT

The scenario impact assessment focused on three dimensions: (1) terrestrial (i.e., change in land use/cover and sediment export), (2) water quality (i.e., change in TSS), and (3) marine (coral reef habitat areas exposed to TSS). First, we assessed and compared the difference between future scenarios and present (baseline) land uses, in particular forest cover. The forest cover change was summarized at the island and watershed scales. Second, we assessed and compared the difference between future scenarios and the present (baseline) in terms of sediment export ($t.yr^{-1}$). The sediment export differences between future scenarios and the present (baseline) was summarized at the island and watershed scales. Third, we assessed and compared the change in TSS in terms of significant increase and change in spatial extent of the plume (footprint area). To do so, we calculated the significant differences in TSS per grid cell, compared to present conditions using the SigDiff function from the R package SDMTools (Januchowski et al. 2010). For each scenario, the grid cells representing significant differences were reclassified to indicate where TSS was significantly different from present conditions ($\alpha = 0.10$). The areas of significant change were converted into a mask to identify coral reef habitat at risk of significant change in TSS across the seascape. For the difference between future scenarios and the present (baseline) in terms of spatial extent of the plume, the areas that were exposed to sediment only under future scenarios were converted into a mask to identify coral reef habitat newly exposed to TSS (Rude et al. 2016).

Lastly, we used the existing coral reef habitat map (Andrefouet et al. 2006) to quantify the coral reef habitat areas (km^2) exposed to change in TSS in terms of significant increase and new exposure. Prior undertaking the overlay analysis, specific coral reef habitat classes that were unlikely to support live corals were removed. The classes removed were: 'land on reef', 'main land', 'undetermined envelope', 'aquatic land feature', 'deep terrace with constructions', 'enclosed basin', 'shelf slope', 'deep drowned reef flat'. In addition, we also combined habitat classes with similar definitions, including:

- shallow lagoon with constructions + shallow lagoonal terrace + shallow lagoonal terrace with constructions
- shallow terrace + shallow terrace with constructions
- enclosed lagoon with constructions + enclosed lagoon
- reticulated fringing + reef flat

2.7 NATIONAL WATERSHED PRIORITIZATION

In order to locate the most effective areas to prioritize forest conservation (i.e., prevent deforestation) to foster coral reef resilience, we linked the coral reef areas vulnerable to sediment runoff from land areas within watersheds upstream that contributed the major portion of the sediment load to those areas. Using the individual watershed sediment plume maps (100 m × 100 m) from the water quality model, we identified the watersheds contributing the majority of sediment runoff to coral reef areas likely to change under land-use change scenarios, compared to present conditions. To do so, we linked the coral reef areas exposed to significant differences in TSS to the watersheds upstream, which contributed the majority (>40%) of the total sediment load (represented by TSS) at those areas in R and ArcGIS. The linked coral reef areas and watersheds were then combined into a single map to display the ridge-to-reef connections under each land-use change scenario.

The 100 watersheds found to have the greatest potential impact on downstream coral reefs were used to determine priority areas on land for conservation. Using the sediment export maps (30 m x 30 m) from the SDR models, we identified land areas contributing the most sediment runoff in each watershed to coral reef areas likely to change under land-use change scenarios, compared to present conditions. We calculated the significant differences in sediment export in the linked watersheds per grid cell, compared to present conditions using the SigDiff function (Januchowski et al. 2010). For each scenario, the grid cells representing significant differences were reclassified to indicate where sediment export was significantly different from present conditions ($\alpha = 0.10$). In ArcGIS, we created a 100 m buffer around those priority land areas based on conservation and logging best management practices (Fischer and Fischenich 2000, McIntosh 2013, Delevaux et al. 2018). To visually represent those results, the priority land areas for each land-use change scenario were combined into a single map to display where conservation and/or restoration actions could foster coral reef resilience.

3. RESULTS

3.1 RIDGE-TO-REEF BASELINE MODELING

Currently, the majority of land use across Vanuatu is made up of forest (82.3%), grassland (10.4%), plantation (6.2%) (e.g., bananas, coconut, cassava, yam), human settlement (0.3%), volcanic ash plain (0.6%), and pine plantation (0.1%) (Fig 3 & Table S1). At the island scale, the forest habitat is most abundant on Santo (29.7%) and Malekula (17.2%). Topographically, Ambae, Santo, Pentecost, and Ambrym are the highest islands (> 300 m), while Aore, Teguna, and Malo are the lowest ones (< 100 m) (Table 2 & Fig S1.1-13). In terms of rainfall, the wettest islands are Teguna and Vanua Lava (> 300 mm/yr) and the driest islands are Aneityum, Tanna, and Erromango (< 200 mm/yr) (Table 2 & Fig S1.14-26). The largest watersheds are found on Santo, Erromango, and Malekula (> 25 km^2) and the smallest on Aore, Teguna, and Tongoa (< 10 km^2) (Table 2 & Fig 2). Downstream, the coral reef habitat area spread across 580 km^2 in the form of mostly narrow reef systems (Fig S2), which drop off quickly into deep water (Fig S3.1). The islands with the most extensive reef habitat are Malekula, Santo, and Efate (Table 2).

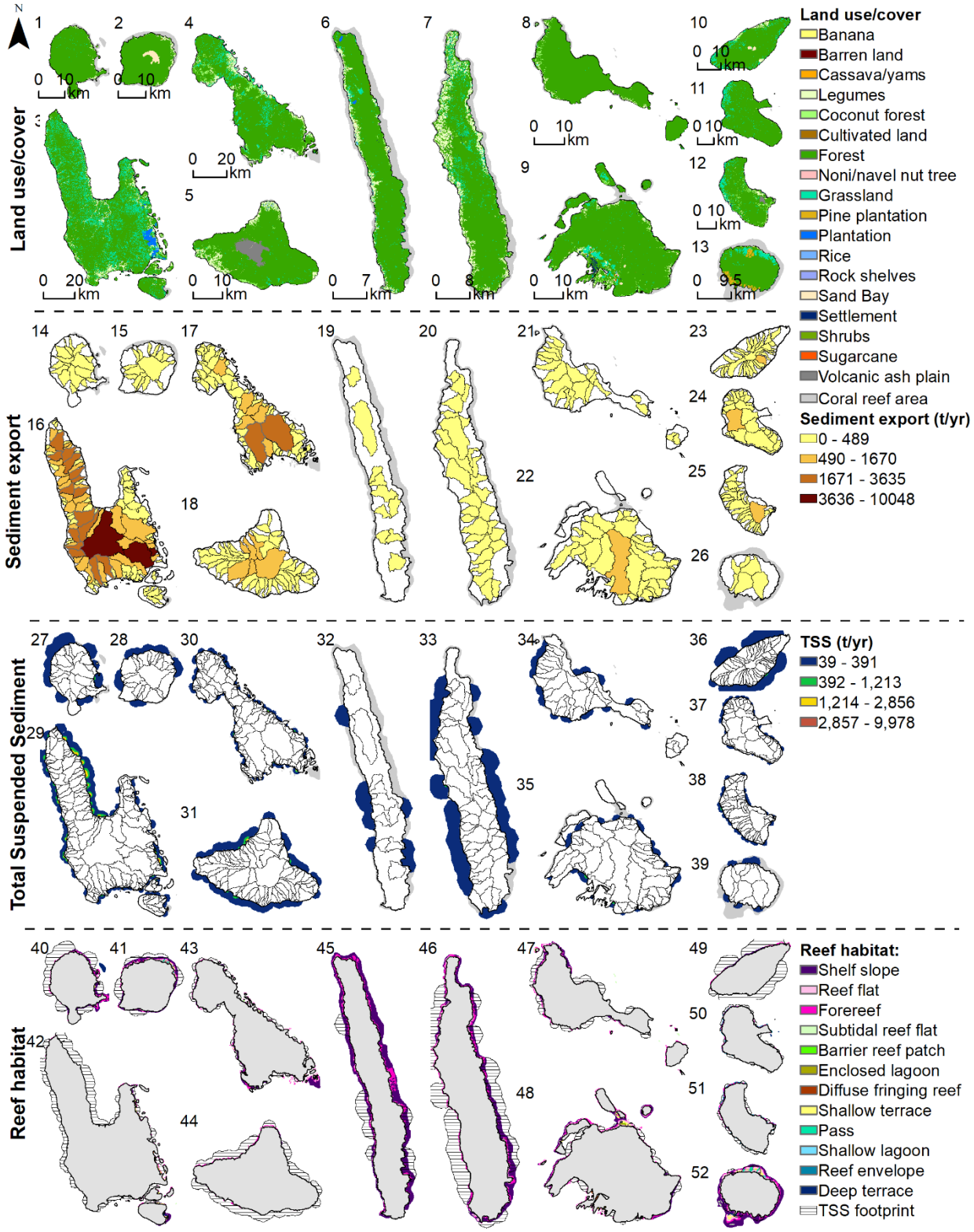

Fig 3. Present ridge to reef model. (1-13) Present land use/cover, (14-26) InVEST SDR results - sediment export (t. yr^{-1}) summarized by watershed, (27-39) modeled TSS plumes (t. yr^{-1}), and (40-52) coral reef habitats exposed to modeled TSS.

Table 2. Present (baseline) ecological and geographic attributes by island. Forest cover (km^2 and %), average elevation (m), rainfall (mm. yr^{-1}), and watershed size (km^2), total sediment export (t. yr^{-1}), and reef habitat area (km^2) by island under present land use/cover.

Islands	Forest		Elevation*	Rainfall*	Watershed size*	Sed	Reef
	km^2	%	m	mm. yr^{-1}	km^2	t. yr^{-1}	km^2
Ambae	347.8	3.6	507.5	287.6	8.2	4627	9.8
Ambrym	555.9	5.8	331.7	257.1	12.1	7930	13.1
Aneityum	132.5	1.4	272.8	193.5	13.3	1079	33.7
Aore	46.1	0.5	49.2	222.9	6.9	0	9.5
Efate	808.3	8.4	148.9	203.0	22.1	2868	68.9
Epi	423.6	4.4	200.1	226.4	12.8	1564	24.9
Erromango	821.2	8.6	227.3	191.7	27.6	3800	25.8
Gaua	281.0	2.9	293.1	296.6	11.3	815	25.1
Maewo	263.6	2.7	252.7	263.3	9.6	767	28.0
Malekula	1687.2	17.6	205.2	230.6	26.5	16200	124.0
Malo	159.0	1.7	86.4	232.3	16.1	49	15.4
Pentecost	371.6	3.9	305.2	259.1	10.3	4938	41.3
Santo	2848.1	29.7	370.7	269.4	36.5	92161	71.9
Tanna	462.0	4.8	271.7	188.6	13.3	2886	23.7
Teguna	26.7	0.3	76.7	309.8	6.9	0	27.1
Tongoa	39.4	0.4	167.4	211.5	5.8	0	5.6
Vanua Lava	320.0	3.3	289.4	307.3	13.3	1444	31.5
Total	*9593.8*	*100*	*238.6**	*244.2**	*14.9**	*141128*	*579.3*

**Represent average values*

As a result of those specific geographies, the sediment export model under the present land use resulted in a total of 141,128 t. yr^{-1} (or 16.1 t/km^2/yr), and sediment export ranged from 0 – 10,048 t. yr^{-1} at the watershed scale. When standardized by the watershed area, the sediment export averages 0 – 2.8 t/ha/year. At the island scale, sediment export is the highest on Santo, followed by Malekula, and Ambrym, which together contribute over 82% of the total sediment load (Table 2). At the watershed scale, watersheds discharging between 2,000-10,000 t. yr^{-1} of sediment are located on Santo (12 watersheds, Fig 3.16) and Malekula (2 watersheds, Fig 3.17), totaling approximately 51,800 t. yr^{-1}, thereby contributing over 36% of the total sediment load. This is due to the presence of the largest watersheds and highest human population on those islands.

Consequently, the terrestrial driver (represented by TSS) ranges from 0 to 9,978 t/yr and showed higher values of suspended sediment along the windward northern and southern side of Santo (Fig 3.29) and along the windward side of Malekula (Fig 3.30). In terms of marine conditions, depth increases very quickly in the study area and ranges from 0 – 967 m (Fig S2.1). The reef habitats with the greatest areas are the forereef and reef flat (Table 3). 30% of all coral reef area in Vanuatu is currently subject to TSS, particularly the forereef and reef flat habitats (Table 3 and Fig 3.40-52).

Table 3. Coral reef habitats exposed to TSS under present land use/cover. Total coral reef habitat area (km^2 and %), coral reef area exposed to TSS under present land use/cover (km^2 and % from total area).

Coral reef habitat type	Total area		Area exposed to TSS	
	km^2	%	km^2	%
Barrier reef pinnacle/patch	1.2	0.2	0.5	0.1
Diffuse fringing reef	5.2	0.7	1.7	0.2
Forereef	352.1	50.1	108.1	15.4
Reef flat	286.7	40.8	86.3	12.3
Shallow lagoon	14.2	2.0	0.0	0.0
Shallow terrace	34.9	5.0	13.2	1.9
Subtidal reef flat*	8.1	1.2	1.0	0.1
Total	*702.3*	*100*	*210.9*	*30.0*

3.2 RIDGE-TO-REEF SCENARIO MODELING

Under the low deforestation scenario, human land use and agriculture land was expanded by 2,606 km^2, resulting in a loss of 27% of forest habitat (Table 4). At the island scale, the forest habitat loss is highest on Santo (Fig 4.3), Efate (Fig 4.9), and Malekula (Fig 4.4) (Table 4). Correspondingly, the sediment models indicated an additional 274,690 t. yr^{-1} (47.5 t/km^2/yr), equivalent to an increase of 195% relative to the baseline in sediment export to the shoreline. When standardized by the watershed area, the sediment export averaged 0 – 3.6 t/ha/year. At the island scale, the relative increase in sediment export is the highest on Santo, followed by Malekula (, and Efate, which together contribute over 57% of the total additional sediment load (Table 4).

At the watershed scale, 30 watersheds accounted for 36% (or 98,298 t. yr^{-1}) of the total sediment increase. Those contributed an additional sediment load ranging from 2,000 to 9,000 t. yr^{-1} and are located on Santo (10 watersheds, Fig 4.16), Malekula (8 watersheds, Fig 4.17), Efate (5 watersheds, Fig 4.22), Erromango (4 watersheds, Fig 4.24), Vanua Lava (2 watersheds, Fig 4.14), and Tanna (1 watershed, Fig 4.25).

Consequently, the increase in sediment export, led to a significant increase in TSS around most islands ranging between 0 – 17,129 t. yr^{-1}, with a net increase ranging between 0 – 8,534 t. yr^{-1}. The change in TSS was higher along the windward and southern side of Santo (Fig 4.29), and along the east side of Malekula (Fig 4.30), as well as around Efate (Fig 4.35).

Table 4. Land and marine indicators change under the low deforestation scenario at the island scale. Forest cover loss (km^2 and %), sediment export increase (t. yr^{-1} & % change relative to baseline), reef habitat exposed to TSS (km^2 & % relative to baseline for modeled islands).

Indictors	**Forest habitat**		**Sediment export**		**Reef habitat**	
Units	***-km²***	***%***	**+ t. yr^{-1}**	**+ %**	***km²***	***%***
Ambae	16.3	0.2	2293	1.6	5.5	0.9
Ambrym	169.4	1.8	20486	14.5	10.9	1.9
Aneityum	16.3	0.2	2745	1.9	12.9	2.2
Aore	38.1	0.4	0	0.0	3.6	0.6
Efate	414.5	4.3	30036	21.3	20.7	3.6
Epi/Tongoa	121.7	1.2	10913	7.7	9.7	1.7
Erromango	186.9	1.9	20623	14.6	12.8	2.2
Gaua	65.7	0.7	10791	7.6	20.0	3.5
Maewo	64.5	0.7	2061	1.5	6.1	1.1
Malekula	332.3	3.5	49617	35.2	40.6	7.0
Malo	117.8	1.2	2434	1.7	7.4	1.3
Pentecost	65.2	0.7	12797	9.1	26.1	4.5
Santo	774.2	8.1	78101	55.3	35.8	6.2
Tanna	160.4	1.7	21537	15.3	14.8	2.6
Vanua Lava	62.7	0.7	10256	7.3	16.2	2.8
Total	*2606*	*27*	*274690*	*194.6*	*243.1*	*42*

Correspondingly, the marine impact assessment revealed that 243 km^2 out of 580 km^2 (or 42%) of coral reef habitat around modeled islands is subject to TSS. At the island scale, the largest areas of coral reef exposed to TSS are located around Malekula, Santo, and Pentecost (Table 4). At the national scale, the main reef habitats exposed to TSS are the forereef, the reef flat, and the shallow terrace (Table 5). When focusing on coral reef areas exposed to a significant change in TSS, the areas subject to TSS are equal to 135.5 km^2 (19.3% of total habitat), particularly for the forereef, reef flat, and shallow terrace (Fig 4.40-52 and Table 5).

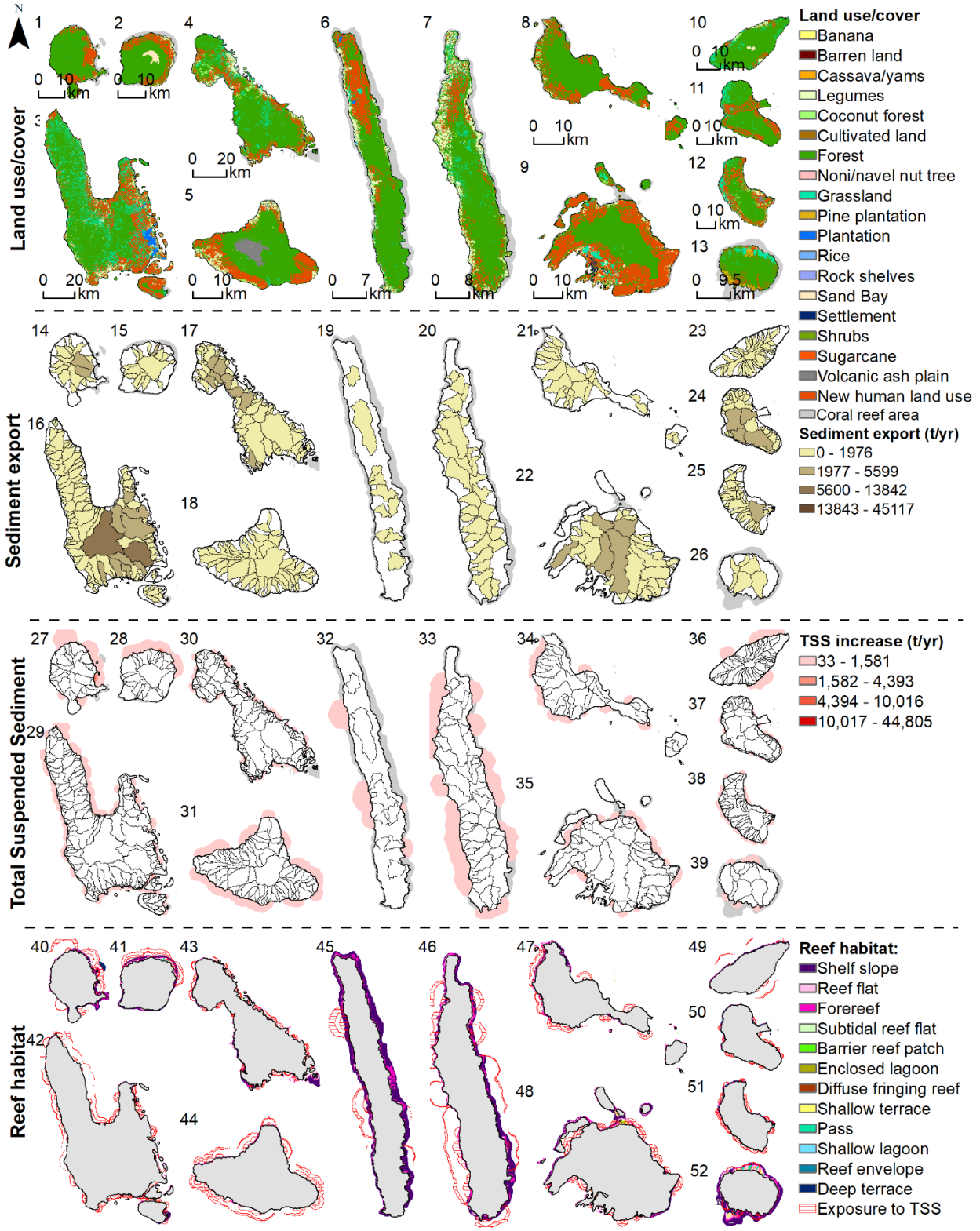

Fig 4. Ridge to reef modeling under the low deforestation scenario. (1-13) Low deforestation scenario land use/cover, (14-26) InVEST SDR results - sediment export (t. yr^{-1}) summarized by watershed, (27-39) modeled TSS plumes (t. yr^{-1}), and (40-52) coral reef habitats exposed to modeled TSS.

Table 5. Coral reef habitats exposed to TSS under the low deforestation scenario.

Total coral reef habitat area exposed to TSS (km^2 and % relative to baseline) and coral reef habitat areas exposed to change in TSS in terms of significant increase and newly exposed (km^2 and % relative to national baseline).

Habitat type	Area exposed to TSS			
	km^2	**%**	**$km^{2\#}$**	**%$^{\#}$**
Barrier reef pinnacle/patch	0.6	0.1	0.2	0.0
Diffuse fringing reef	1.9	0.3	1.3	0.2
Forereef	128.9	18.4	66.5	9.5
Reef flat	104.1	14.8	56.1	8.0
Shallow terrace	16.6	2.4	10.4	1.5
Subtidal reef flat*	1.7	0.2	1.1	0.2
Total	*253.8*	*36.1*	*135.5*	*19.3*

[#] Values represent coral habitat newly exposed to a statistically significant change in TSS.

Under the high deforestation scenario, human settlement and agriculture land was expanded by 4,050 km^2, resulting in a loss of 42% of forest habitat (Table 6). At the island scale, the forest habitat loss was highest on Santo (Fig 5.3), Efate (Fig 5.9), and Malekula (Fig 5.4) (Table 6). Correspondingly, the sediment models indicated an additional 1,160,196 t. yr^{-1} of sediment discharging at the shoreline (i.e., total sediment load = 1,301,324 t. yr^{-1}, equivalent to 148.6 t/km^2/yr). When standardized by watershed area, the sediment export averaged 0 – 9.1 t/ha/year. At the island scale, the relative increase in sediment export was highest on Santo, followed by Malekula, and Tanna, which together contributed over 53% of the total sediment load (Table 6). At the watershed scale, 29 watersheds contributed an increase in sediment between 8,000-50,000 t/yr (accounting for 32% increase or 376,559 t. yr^{-1}) and those are located on Santo (12 watersheds, Fig 5.16), Malekula (8 watersheds, Fig 5.17), Pentecost (3 watersheds, Fig 5.20), Erromango (2 watersheds, Fig 5.24), Vanua Lava (2 watersheds, Fig 5.14), Tanna (1 watershed, Fig 5.25), and Aneityum (1 watershed, Fig 5.26). Consequently, the increase in sediment export led to a significant increase in TSS around most islands ranging between 0 – 54,782 t. yr^{-1}, with a net increase ranging between 0 – 44,805 t. yr^{-1}. The change in TSS was highest along the windward and leeward side of Santo (Fig 5.29), along the east and north side of Malekula (5.30), around Efate (Fig 5.35), and Pentecost (Fig 5.33).

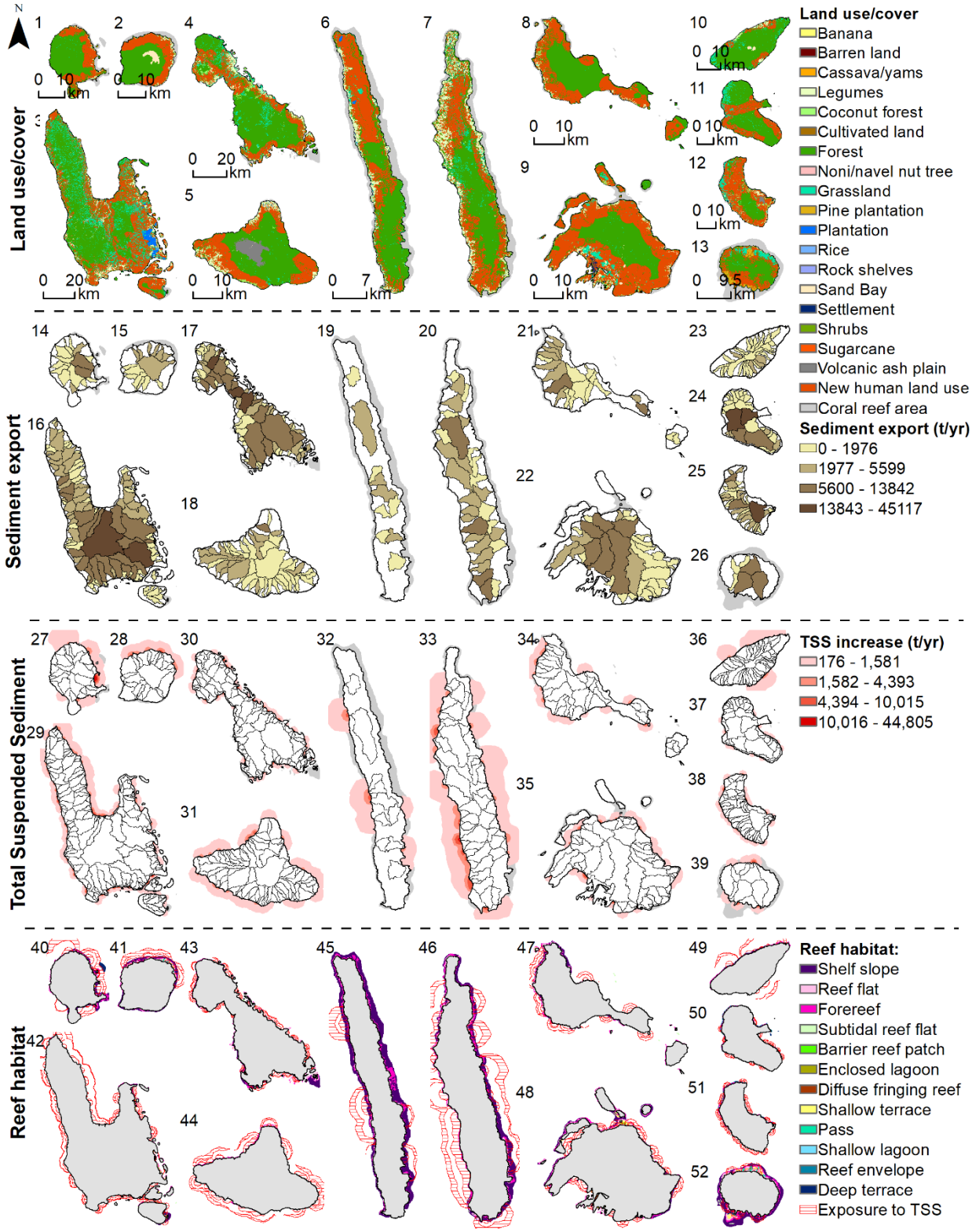

Fig 5. Ridge to reef modeling under the high deforestation scenario. (1-13) Low deforestation scenario land use/cover, (14-26) InVEST SDR results – sediment export (t. yr^{-1}) summarized by watershed, (27-39) modeled TSS plumes (t. yr^{-1}), and (40-52) coral reef habitats exposed to modeled TSS.

Table 6. Land and marine indicators change under the high deforestation scenario at the island scale. Forest cover loss (km^2 and %), sediment export increase (t. yr^{-1} & % change relative to baseline), reef habitat exposed to TSS (km^2 & % relative to baseline for modeled islands).

Islands	**Forest habitat**		**Sediment export**		**Reef habitat**	
Units	**-km^2**	**-%**	**+ t. yr^{-1}**	**%**	**km^2**	**%**
Ambae	39.3	0.4	20343	14.4	5.6	1.0
Ambrym	224.0	2.3	56289	39.9	11.2	1.9
Aneityum	56.4	0.6	27760	19.7	15.8	2.7
Aore	41.7	0.4	0	0.0	3.9	0.7
Efate	503.3	5.2	72403	51.3	22.1	3.8
Epi/Tongoa	211.8	2.2	47997	34.0	10.3	1.8
Erromango	289.7	3.0	63872	45.3	13.3	2.3
Gaua	109.1	1.1	26492	18.8	20.2	3.5
Maewo	127.2	1.3	15278	10.8	6.6	1.1
Malekula	563.8	5.9	228559	162.0	44.7	7.7
Malo	125.1	1.3	3389	2.4	7.5	1.3
Pentecost	175.4	1.8	99893	70.8	27.8	4.8
Santo	1156.3	12.1	376342	266.7	36.7	6.3
Tanna	317.1	3.3	86235	61.1	15.9	2.7
Vanua Lava	109.5	1.1	35345	25.0	17.4	3.0
Total	*4050*	*42*	*1160196*	*822.1*	*259.0*	*44.7*

Correspondingly, the marine impact assessment revealed that 259 km^2 out of 580 km^2 (or 44.7%) of coral reef habitats around modeled islands were subject to TSS. At the island scale, the largest areas of coral reefs exposed to TSS are located around Malekula , Santo, and Pentecost (Table 6). At the national scale, the main reef habitats exposed to TSS are the forereef, the reef flat, and the shallow terrace (Table 7). When focusing on coral reef areas exposed to a significant change in TSS, the areas are equal to 166 km^2 (or 23.6%), particularly for forereefs, reef flats, and shallow terrace (Table 7 & Fig 5.40-52).

Table 7. Coral reef habitats exposed to TSS under the high deforestation scenario. Total coral reef habitat area exposed to TSS (km^2 and %) and coral reef habitat areas exposed to change in TSS in terms of significant increase and newly exposed (km^2 and % relative to baseline).

Habitat type	Area exposed to TSS			
	km^2	**%**	**$km^{2\#}$**	**%#**
Barrier reef pinnacle/patch	0.7	0.1	0.5	0.1
Diffuse fringing reef	1.9	0.3	1.4	0.2
Forereef	136.6	19.5	81.8	11.6
Reef flat	111.5	15.9	69.3	9.9
Shallow terrace	17.3	2.5	11.6	1.7
Subtidal reef flat*	2.0	0.3	1.4	0.2
Total	*270.0*	*38.4*	*166.0*	*23.6*

Values represent coral habitat newly exposed to a statistically significant change in TSS.

3.3 IDENTIFYING PRIORITY LAND-SEA CONNECTIONS

Where a significant change was detected within and along the edge of the TSS plumes on coral reef habitat under the low deforestation scenario, 261 watersheds were identified as a source of risk for downstream coral reefs and contained land areas where the change in sediment export was significantly different (Fig 6.1-13). The reef areas (showing only the connections for the watersheds contributing the largest change in TSS) were located directly downstream from the watersheds experiencing deforestation which were ranked based on area of coral reefs potentially affected (Fig 6.14-26). The 100 watersheds contributing to the largest areas of impacted coral reefs downstream were selected as priority watersheds. Land areas where the change in sediment export was significantly different from present conditions were selected as priorities for conservation to prevent sediment runoff (Fig 6.27-39).

Priority watersheds were identified on nearly all the islands modeled. Several island regions are notable in terms of the number of priority watersheds that could potentially impact coral reefs though sedimentation. These include the northeast part of Santo Island (Fig 6.29), northern Gaua (Fig 6.28), north Pentecost (Fig 6.33), and west Epi (Fig 6.34). Efate had priority watersheds discharging sediments on each side of the island with a notably large area of vulnerable coral reefs to the north (Fig 6.35). Tagabe watershed was also selected as a priority, however, it was not among the top 100. Among the modeled islands, Ambae (Fig 6.36) and Ambrym (Fig 6.31) had the least number of priority watersheds. Areas within each priority watershed which contributed the most to sedimentation were also identified.

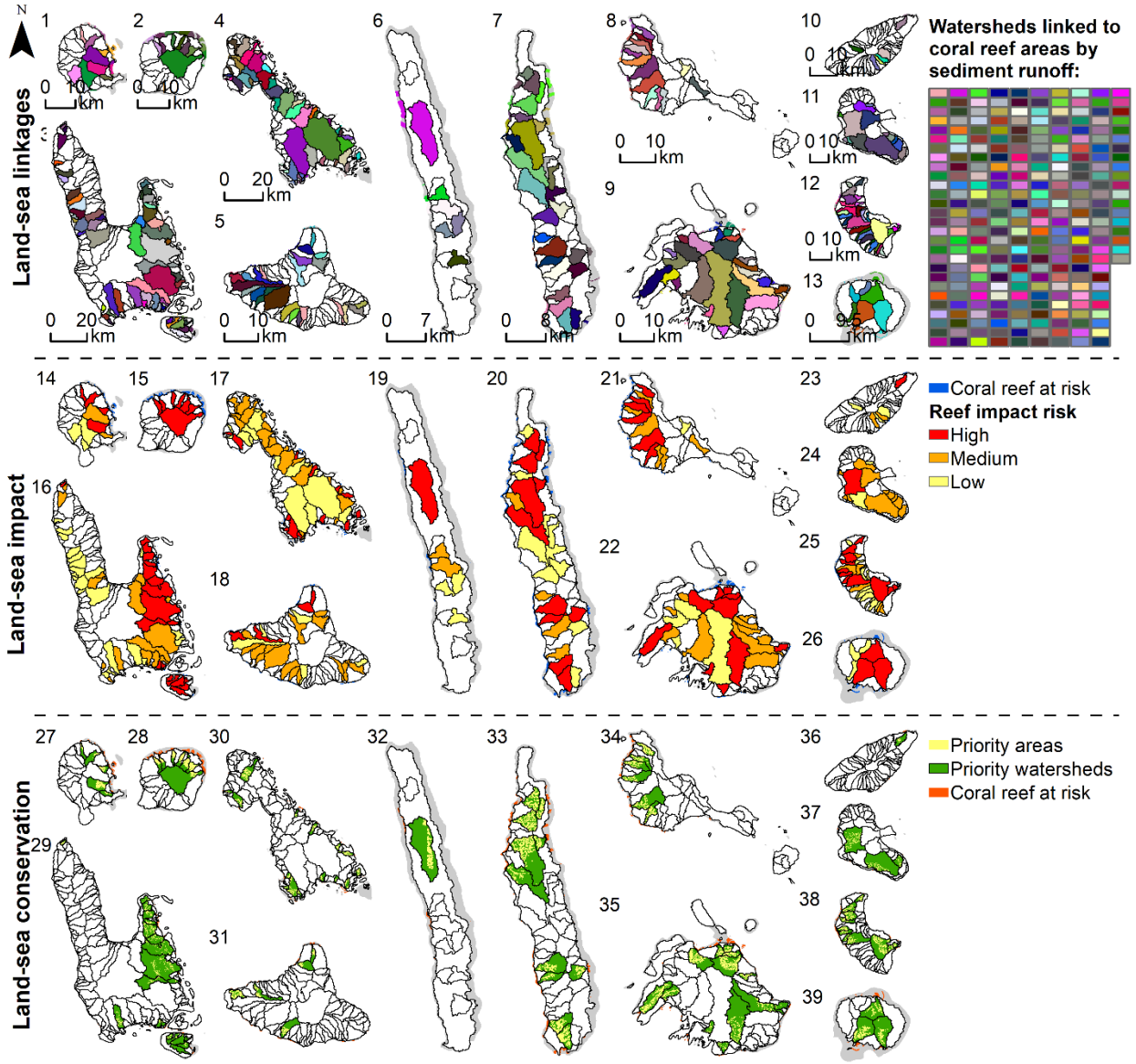

Fig 6. Key ridge-to-reef connections under the low deforestation scenario. (1-13) Watersheds linked to coral reef areas vulnerable to their sediment runoff are indicated by matching colors. (14-26) Ridge-to-reef connections are ranked by the total area of coral reef habitat potentially at risk, and (27-39) top 100 priority watersheds where conservation (i.e., avoiding deforestation) can benefit the largest areas of coral reef are indicated in green, priority areas for conservation actions within watersheds are shown in yellow, and coral reef areas vulnerable to human impacts under the low deforestation scenario are shown in orange.

Where a significant change was detected within and along the edge of the TSS plumes on coral reef habitat under the high deforestation scenario, 274 watersheds were identified as a source of risk for downstream coral reefs and contained land areas where the change in sediment export was significantly different (Fig 7.1-13). Like the low deforestation scenario, the reef areas (showing only the connections for the watersheds contributing the largest change in TSS) are located directly downstream from the watersheds experiencing deforestation which were ranked based on area of coral reefs potentially affected (Fig 7.14-26). The 100 watersheds contributing to the largest areas

of impacted coral reefs downstream were selected as priority watersheds. Land areas where the change in sediment export was significantly different from present conditions were selected as priorities for conservation to prevent sediment runoff (Fig 7.27-39).

Locations of priority watersheds identified using the high deforestation scenario were very similar to those identified with the low deforestation scenario with additional watersheds identified as priorities. Island regions which included a number of priority watersheds include the northeast part of Santo Island (Fig 7.29), northern Gaua (Fig 7.28), north Pentecost (Fig 7.33), west Epi (Fig 7.34), and north Efate (Fig 7.35). Tagabe watershed on Efate Island was also selected as a priority, however, it was not among the top 100. Among the modeled islands, Ambae (Fig 7.36) and Ambrym (Fig 7.31) had the least number of priority watersheds. Areas within each priority watershed which contributed the most to sedimentation were also identified.

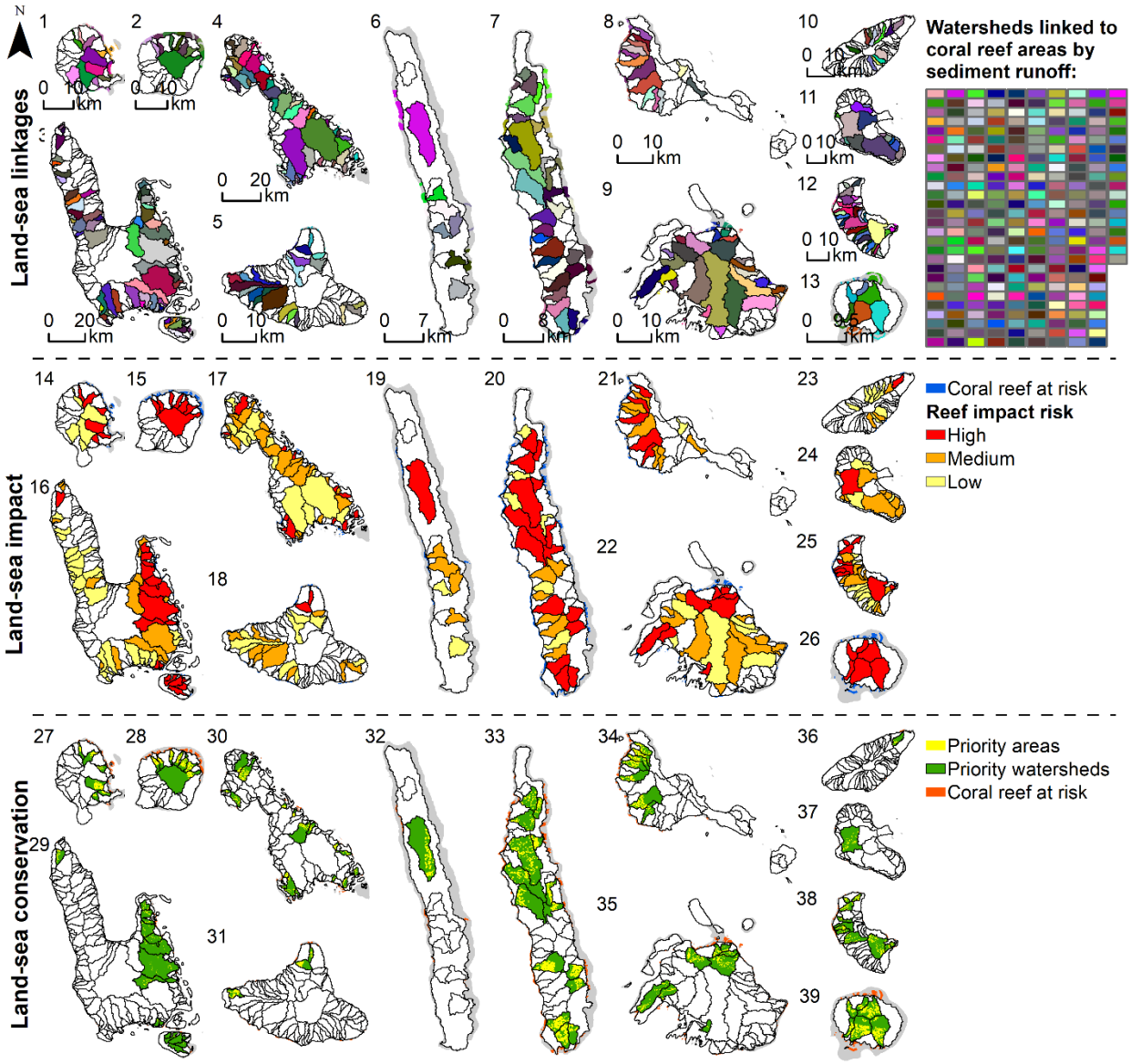

Fig 7. Key ridge-to-reef connections under the high deforestation scenario. (1-13) Watersheds linked to coral reef areas are indicated by matching colors. Under the high deforestation scenario, watersheds are linked to coral reef areas vulnerable to their sediment runoff. (14-26) Ridge-to-reef connection are ranked by the total area of coral reef habitat potentially at risk, and (27-39) priority watersheds where conservation (i.e., avoiding deforestation) can benefit coral reef areas are indicated in green, and priority areas for conservation actions within watersheds are shown in yellow and coral reef areas vulnerable to human impacts under the high deforestation scenario are shown in orange.

4. DISCUSSION

This ridge-to-reef decision support tool identified reef areas vulnerable to land use/cover change and pinpointed land areas where forest conservation could benefit terrestrial and downstream marine ecosystems. The modeling tool was first informed by data layers representing current conditions and these results represent the effect of current land-use on sediment runoff once it enters the nearshore environment. Then, land-use change scenarios were applied to quantify the potential impact of TSS on reefs under increasing levels of development and deforestation. The scenario analysis results identified ~ 200 watersheds (out of 411 modeled watersheds), where forest conservation can reduce TSS risk to downstream coral reefs (Figs 6 & 7). In Vanuatu, the reef areas (showing only the connections for the watersheds contributing the largest change in TSS) are located directly downstream from the watersheds experiencing deforestation. Therefore, conserving forest in priority land areas of these key watersheds not only maintains good water quality essential for healthy coral reefs, it is also an important management strategy to mitigate the impacts of climate change on coral reefs within the range of sediment dispersal from river plumes (Szmant 2002).

The adverse direct and indirect impacts of sedimentation and turbidity on benthic habitat at local scales has been well established (Fabricius 2005a). Increases in sediment can indirectly hinder competition for space by reef calcifiers (Smith et al. 2016a). Although coral reefs can flourish in turbid waters (Anthony 1999), they are typically restricted to shallow waters (4–10 m) (Yentsch et al. 2002, Fabricius et al. 2005), and generally support fewer species, slower growth rates, and poorer recruitment (Rogers 1990). Coral reef fishes can also be adversely affected by sedimentation and turbidity directly through altered foraging (Johansen and Jones 2013) and indirectly by altering the benthic community structure and composition (Rogers 1990). The degree of dependence with respect to the effects of terrestrial run-off on different benthic groups may influence the susceptibility of fishes to habitat impacts from sediment runoff (Brown et al. 2017c), which can decrease or alter fish recruitment (DeMartini et al. 2013, Wenger et al. 2014). Based on these established impacts, we assumed that increase in TSS over coral reef habitat negatively affects live coral cover and reef fish biomass to prioritize land areas for conservation.

Coral reef areas constitute important local fishing grounds for nearby coastal villages (Eriksson et al. 2017). To foster the resilience of these reefs, it is essential to consider minimizing land-based impacts, as research increasingly shows that marine closures are less effective when exposed to high land-based source pollution (Halpern et al. 2013a, Wenger et al. 2015). By gaining knowledge of where soils are more likely to erode under land-use change, we can inform where conservation actions on land or sustainable land-use practices can provide benefits downstream. Conservation planning should design protected areas that go beyond protecting parts of the ecosystem within their boundaries and instead augment resilience on a scale that transcends land-sea boundaries (Game et al. 2008). These results can inform ridge-to-reef management which requires coordinating across different agencies. In Vanuatu, the Fisheries Department and the Department of Environmental Protection and Conservation have authority over coral reef ecosystems and the

Department of Forests is mandated with the management of the forest sector throughout Vanuatu. The Department of Forests is mandated with the management of the forest sector. The mismatch of governance and natural boundaries/processes can result in decision-makers having no control over activities outside their jurisdiction that impact the ecology of their systems (Jupiter et al. 2014). These results can facilitate discussions across agencies and inform stakeholders. The outputs are simple maps and spreadsheets, thereby allowing for more transparency in the decision-making process, which can foster community buy-in (Bremer et al. 2015).

This decision support tool was developed and implemented in a data-poor region and therefore under several key data gaps and caveats. First, the resolution of the input foundational layers, including the soils (~900 x 900 m), rainfall (~900 x 900 m), bathymetry (~500 x 500 m), and currents (9 x 9 km), are coarse resolution for some of the small islands found in Vanuatu. Because soil and rainfall maps are coarser resolution than the DEM input, at which SDR operates, it may obscure small scale processes and spatial nuances which can occur in small watersheds and narrow reef systems often found in tropical oceanic island environments (Delevaux et al. 2019). In addition to the low resolution, it is also important to note that the bathymetry and current maps were interpolated nearshore to fill in the gaps along the shoreline, which may create erroneous values. This may impact the dispersion of the TSS plumes in some regions. For instance, the coastal plume models could over- or under-estimate the TSS proxy values because we could not account for the effect of fine scale marine topography or tidal-driven transport on sediment dispersal and settling rates due to lack of data.

In terms of data gaps, no in situ water quality data was available for the streams and coastal waters modeled, which prevented us from ground-truthing the sediment and coastal plume models. The sediment loadings for each watershed may have under-estimated some sediment export loads due to erosion processes that we did not account for in our modeling approach, such as land slip and stream bank erosion which can be major sources of sediment (Olley et al. 2015, Brown et al. 2017a). Landslides additionally represent a potentially large and unexplored source of fine sediment in Vanuatu. Approximately 78% of Vanuatu is reported to be above 18 degrees slope, which some authors use as a threshold for instability (Morrison et al. 1990). Deforestation on steep slopes has the potential to catastrophically destabilize large areas because of the role that roots can play in binding shallow (e.g. 2–3 m) subsurface soils (Morrison et al. 1990).

Future work should investigate how these modeled plumes of TSS compare to local knowledge from coastal communities, satellite imagery, and/or in-situ data as those become available. In addition, future research should focus on generating more refined bathymetry data using satellite imagery (Knudby et al. 2011, Roelfsema et al. 2013), which can help refine the plume dispersion models and provide input layers for species distribution modeling. In the meantime, spatial planning requires information to prioritize efforts on that ground and these global datasets are freely available for data poor regions such as Vanuatu. Additionally, spatial prioritization requires spatial consistency in the datasets used, otherwise conservation actions tend to focus efforts in data

rich places. The global data inputs used in this analysis provide consistent coverage of the entire archipelago.

This research identified where coral reef areas may be subject to sediment exposure, but did not explicitly model potential interactions with nutrients, fishing pressure, or climate change and cumulative impacts due to a lack of data and the poor understanding of those processes (Anthony 2006, Wenger et al. 2015, Morgan et al. 2016). It is increasingly recognized that water quality in combination with elevated sea surface temperatures (SST) can have a profound influence on management outcomes of nearshore coral reefs under climate change (Anthony et al. 2007). Recent work has shown that sediments can have an antagonistic effect with SST by mitigating bleaching impacts through shading (Anthony 2006, Anthony et al. 2007), while other research has shown that excess nutrients or fishing pressure can prevent recovery from climate change impacts (Wooldridge 2009b, Wilson et al. 2010).

We tested how sensitive our modeling framework was to the linkages between the SDR model and the plume models by running the framework with various c-factor values for the major land-use types. We observed that the magnitude of change and the sizes of the spatial footprints of coral reef impacts as a function of sediment runoff varied depending on the c-factors used. However, the locations of coral reef impact from sediment runoff were consistently detected near the watersheds that contributed the largest change in sediment export. Therefore, the priority areas on land within watersheds linked to coral reef areas at risk did not change. Future policy discussion will use these trends to identify priority sites for further field investigations and/or conservation actions

5. CONCLUSION

Ridge-to-reef management requires the ability to trace where land-based pollutants come from and where they are likely to cause an impact once they enter the marine environment. This project adapted, applied and scaled up a linked land-sea decision support tool (Delevaux et al. 2018), to quantify, track, and map the impact of land-use change on coral reefs at the sub-watershed scale. This approach leveraged existing data, reducing the amount of time and resources needed to characterize priority areas. The soils, rainfall, bathymetry, and current data used in this study are derived from global datasets, freely available, making this approach useful for regions with limited resources. The field data used to conduct the marine impact assessment was collected by SPC and the monitoring programs of local government agencies. The terrestrial and marine habitat maps were provided by SPC GEM. In addition, this modeling framework relies on two freely available software packages (i.e., InVEST SDR, and R) and the proprietary software ArcGIS (also available with open access QGIS) (ESRI 2011, R. C. Team 2014, Q. D. Team 2015, Hamel et al. 2015). By coupling this tool with scenario planning, we were able to inform local conservation actions and identify priority areas on land that can foster coral reef resilience.

This information can be used to inform land-sea planning and help prioritize local conservation actions in Vanuatu. By simultaneously evaluating the effect of land-use change, sediment runoff, coral reef habitat, this research highlighted the potential trade-offs and synergies arising between land and sea under different land-use scenarios. Priority watersheds were identified on nearly all the islands modeled along with areas within each priority watershed which can contribute the most to sedimentation and downstream coral reef impacts. This information should be combined with existing land use plans to further prioritize areas for management actions. The next steps would be to build a suite of land-use management scenarios within the priority areas identified in this study. Then, evaluate tradeoffs to identify optimal management solutions. By adopting a ridge-to-reef conservation planning process, protected areas can be designed for multiple benefits that include improvements in biodiversity, drinking water, and reef fisheries. These findings can also help inform priorities for future conservation leases or other payment for ecosystem service schemes by: (1) identifying relevant communities, (2) facilitating communication using maps as visuals, and (3) locating where forest conservation or restoration actions can benefit coral reefs and improve fisheries livelihoods. The implementation of this approach in GIS allows managers to visualize and foresee the potential outcomes of management interventions. This type of approach has the potential to engender collaborative stewardship among agencies, communities, and other stakeholders and inform ecosystem-based, land-sea conservation planning in Vanuatu and other Pacific Island nations.

6. REFERENCES

Alagona, P. S., J. Sandlos, and Y. F. Wiersma. 2012. Past imperfect: using historical ecology and baseline data for conservation and restoration projects in North America. Environmental Philosophy 9:49–70.

Alvarez-Romero, J. G., R. L. Pressey, N. C. Ban, K. Vance-Borland, C. Willer, C. J. Klein, and S. D. Gaines. 2011. Integrated land-sea conservation planning: the missing links. Annual Review of Ecology, Evolution, and Systematics 42:381–409.

Andrefouet, S., F. E. Muller-Karger, J. A. Robinson, C. J. Kranenburg, D. Torres-Pulliza, S. A. Spraggins, and B. Murch. 2006. Global assessment of modern coral reef extent and diversity for regional science and management applications: a view from space. Pages 1732–1745 Proceedings of the 10th International Coral Reef Symposium. Japanese Coral Reef Society Okinawa, Japan.

Anthony, K. R. 1999. Coral suspension feeding on fine particulate matter. Journal of Experimental Marine Biology and Ecology 232:85–106.

Anthony, K. R. 2006. Enhanced energy status of corals on coastal, high-turbidity reefs. Marine Ecology Progress Series 319:111–116.

Anthony, K. R. 2016. Coral reefs under climate change and ocean acidification: challenges and opportunities for management and policy.

Anthony, K. R., S. R. Connolly, and O. Hoegh-Guldberg. 2007. Bleaching, energetics, and coral mortality risk: Effects of temperature, light, and sediment regime. Limnology and oceanography 52:716–726.

Barnett, J. 2011. Dangerous climate change in the Pacific Islands: food production and food security. Regional Environmental Change 11:229–237.

Batjes, N. H. 2016. Harmonized soil property values for broad-scale modelling (WISE30sec) with estimates of global soil carbon stocks. Geoderma 269:61–68.

Bellwood, D. R., T. P. Hughes, C. Folke, and M. Nyström. 2004. Confronting the coral reef crisis. Nature 429:827–833.

Bode, M., K. A. Wilson, T. M. Brooks, W. R. Turner, R. A. Mittermeier, M. F. McBride, E. C. Underwood, and H. P. Possingham. 2008. Cost-effective global conservation spending is robust to taxonomic group. Page Proceedings of the National Academy of Sciences 105:6498.

Borselli, L., P. Cassi, and D. Torri. 2008. Prolegomena to sediment and flow connectivity in the landscape: a GIS and field numerical assessment. Catena 75:268–277.

Braun, C. D., B. Galuardi, and S. R. Thorrold. 2018. HMMoce: An R package for improved geolocation of archival-tagged fishes using a hidden Markov method. Methods in Ecology and Evolution 9:1212–1220.

Bremer, L. L., J. M. Delevaux, J. J. Leary, L. J. Cox, and K. L. Oleson. 2015. Opportunities and strategies to incorporate ecosystem services knowledge and decision support tools into planning and decision making in Hawai ‘i. Environmental management 55:884–899.

Brown, C. J., S. D. Jupiter, S. Albert, C. J. Klein, S. Mangubhai, J. M. Maina, P. Mumby, J. Olley, B. Stewart-Koster, and V. Tulloch. 2017a. Tracing the influence of land-use change on water quality and coral reefs using a Bayesian model. Scientific reports 7:4740.

Brown, C. J., S. D. Jupiter, H.-Y. Lin, S. Albert, C. Klein, J. M. Maina, V. J. Tulloch, A. S. Wenger, and P. J. Mumby. 2017c. Habitat change mediates the response of coral reef fish populations to terrestrial run-off. Marine Ecology Progress Series 576:55–68.

Cavalli, M., S. Trevisani, F. Comiti, and L. Marchi. 2013. Geomorphometric assessment of spatial sediment connectivity in small Alpine catchments. Geomorphology 188:31–41.

Chicas, S., and K. Omine. 2015. Forest Cover Change and Soil Erosion in Toledo's Rio Grande Watershed. ISPRS-International Archives of the Photogrammetry, Remote Sensing and Spatial Information Sciences 40:353–358.

Coreau, A., G. Pinay, J. D. Thompson, P.-O. Cheptou, and L. Mermet. 2009. The rise of research on futures in ecology: rebalancing scenarios and predictions. Ecology Letters 12:1277–1286.

Dauvergne, P. 1998. Globalisation and deforestation in the Asia-Pacific. Environmental Politics 7:114–135.

Delevaux, J. M. S., S. D. Jupiter, K. A. Stamoulis, L. L. Bremer, A. S. Wenger, R. Dacks, P. Garrod, K. A. Falinski, and T. Ticktin. 2018. Scenario planning with linked land-sea models inform where forest conservation actions will promote coral reef resilience. Scientific Reports 8:12465.

Delevaux, J. M., K. A. Stamoulis, R. Whittier, S. D. Jupiter, L. L. Bremer, A. Friedlander, N. Kurashima, J. Giddens, K. B. Winter, and M. Blaich-Vaughan. 2019. Place-based management can reduce human impacts on coral reefs in a changing climate. Ecological Applications 29: e01891.

DeMartini, E., P. Jokiel, J. Beets, Y. Stender, C. Storlazzi, D. Minton, and E. Conklin. 2013. Terrigenous sediment impact on coral recruitment and growth affects the use of coral habitat by recruit parrotfishes (*F. scaridae*). Journal of coastal conservation 17:417–429.

DeVantier, B. A., and A. D. Feldman. 1993. Review of GIS applications in hydrologic modeling. Journal of Water Resources Planning and Management 119:246–261.

Doheny, B., K. Maher, A. Minks, J. Rude, and M. Tyner. 2013. Ridge to Reef: Land Use, Sedimentation, and Marine Resource Vulnerability in Raja Ampat, Indonesia. Page 93. Conservation International and Bren School of Environmental Science and Management, UCSB.

Eckardt, R., M. Herold, J. Sambale, and S. Weaver. 2008. Monitoring deforestation patterns and processes in the Pacific island state of Vanuatu. Page 71 Geospatial crossroads GIForum'08: proceedings of the Geoinformatics Forum Salzburg. Wichmann.

El-Swaify, S. A., E. W. Dangler, and C. L. Armstrong. 1982. Soil erosion by water in the tropics. College of Tropical Agriculture and Human Resources, Univ. of Hawaii Research Extension Series 024, Honolulu.

Eriksson, H., J. Albert, S. Albert, R. Warren, K. Pakoa, and N. Andrew. 2017. The role of fish and fisheries in recovering from natural hazards: lessons learned from Vanuatu. Environmental Science & Policy 76:50–58.

ESRI. 2011. ArcGIS Desktop: Release 10.4. Environmental Systems Research Institute, Redlands, CA.

Evensen, C. I., S. A. El-Swaify, C. W. Smith, and D. Flanagan. 2001. C-Factor development for sugarcane in Hawaii. Pages 687-690. American Society of Agricultural and Biological Engineers, Honolulu, HI, USA.

Fabricius, K., G. De'ath, L. McCook, E. Turak, and D. M. Williams. 2005. Changes in algal, coral and fish assemblages along water quality gradients on the inshore Great Barrier Reef. Marine Pollution Bulletin 51:384–398.

Fabricius, K. E. 2005. Effects of terrestrial runoff on the ecology of corals and coral reefs: review and synthesis. Marine Pollution Bulletin 50:125–146

Falinski, K. A. 2016. Predicting sediment export into tropical coastal ecosystems to Support ridge to reef management. University of Hawaii at Manoa, Honolulu, Hawaii, USA.

FAO. 2007. Strategic environmental assessment. http://www.fao.org/docrep/007/y2413e/y2413e09.htm.

Fick, S. E., and R. J. Hijmans. 2017. WorldClim 2: new 1-km spatial resolution climate surfaces for global land areas. International journal of climatology 37:4302–4315.

Fischer, R. A., and J. C. Fischenich. 2000. Design recommendations for riparian corridors and vegetated buffer strips. Army engineer waterways experiment station vicksburg ms engineer research and development center.

Game, E. T., M. E. Watts, S. Wooldridge, and H. P. Possingham. 2008. Planning for persistence in marine reserves: a question of catastrophic importance. Ecological Applications 18:670–680.

Gholami, L., S. H. R. Sadeghi, and A. V. K. Darvishan. 2009. Modeling storm-wise sediment delivery ratio model in Chehelgazi watershed by using climatic and hydrologic characteristics. Journal of Agricultural Sciences and Natural Resources 16:253–260.

Grorud-Colvert, K., J. Claudet, B. N. Tissot, J. E. Caselle, M. H. Carr, J. C. Day, A. M. Friedlander, S. E. Lester, T. L. De Loma, D. Malone, and others. 2014. Marine protected area networks: assessing whether the whole is greater than the sum of its parts. PLoS One 9:e102298.

Groves, C. R., E. T. Game, M. G. Anderson, M. Cross, C. Enquist, Z. Ferdana, E. Girvetz, A. Gondor, K. R. Hall, and J. Higgins. 2012. Incorporating climate change into systematic conservation planning. Biodiversity and Conservation 21:1651–1671.

Gurney, G. G., J. Melbourne-Thomas, R. C. Geronimo, P. M. Aliño, and C. R. Johnson. 2013. Modelling Coral Reef Futures to Inform Management: Can Reducing Local-Scale Stressors Conserve Reefs under Climate Change? PLOS ONE 8:80137.

Halpern, B. S., K. L. McLeod, A. A. Rosenberg, and L. B. Crowder. 2008a. Managing for cumulative impacts in ecosystem-based management through ocean zoning. Ocean & Coastal Management 51:203–211.

Halpern, B. S., K. A. Selkoe, C. White, S. Albert, and S. Aswani. 2013a. Marine protected areas and resilience to sedimentation in the Solomon Islands. Coral Reefs 32:61–69.

Halpern, B. S., K. A. Selkoe, C. White, S. Albert, S. Aswani, and M. Lauer. 2013b. Marine protected areas and resilience to sedimentation in the Solomon Islands. Coral Reefs 32:61–69.

Halpern, B. S., S. Walbridge, K. A. Selkoe, C. V. Kappel, F. Micheli, and C. D'Agrosa. 2008b. A Global Map of Human Impact on Marine Ecosystems. Science 319:948–952.

Hamel, P., R. Chaplin-Kramer, S. Sim, and C. Mueller. 2015. A new approach to modeling the sediment retention service (InVEST 3.0): Case study of the Cape Fear catchment. North Carolina, USA. Sci. Total Environ.

Hijmans, R. J. 2019. raster: Geographic Data Analysis and Modeling. R package version 2.9-23.

Hoegh-Guldberg, O. 1999. Climate change, coral bleaching and the future of the world's coral reefs. Marine and freshwater research 50:839–866.

Houk, P., D. Benavente, J. Iguel, S. Johnson, and R. Okano. 2014. Coral Reef Disturbance and Recovery Dynamics Differ across Gradients of Localized Stressors in the Mariana Islands. PLOS ONE 9:e105731.

Januchowski, S. R., R. L. Pressey, J. VanDerWal, and A. Edwards. 2010. Characterizing errors in digital elevation models and estimating the financial costs of accuracy. International Journal of Geographical Information Science 24:1327–1347.

Jenkins, A., P. Horwitz, and K. Arabena. 2018. My island home: place-based integration of conservation and public health in Oceania. Environmental Conservation 45:125–136.

Johansen, J. L., and G. P. Jones. 2013. Sediment-induced turbidity impairs foraging performance and prey choice of planktivorous coral reef fishes. Ecological Applications 23:1504–1517.

Jupiter, S. D., A. P. Jenkins, W. J. L. Long, S. L. Maxwell, T. J. Carruthers, K. B. Hodge, H. Govan, J. Tamelander, and J. E. Watson. 2014. Principles for integrated island management in the tropical Pacific. Pacific Conservation Biology 20:193–205.

Jupiter, S. D., A. Wenger, C. J. Klein, S. Albert, S. Mangubhai, J. Nelson, L. Teneva, V. J. Tulloch, A. T. White, and J. E. Watson. 2017. Opportunities and constraints for implementing integrated land–sea management on islands. Environmental Conservation:1–13.

Karydas, C., M. Petriolis, and I. Manakos. 2013. Evaluating alternative methods of soil erodibility mapping in the Mediterranean Island of Crete. Agriculture 3:362–380.

Klein, C. J., S. D. Jupiter, E. R. Selig, M. E. Watts, B. S. Halpern, M. Kamal, C. Roelfsema, and H. P. Possingham. 2012. Forest conservation delivers highly variable coral reef conservation outcomes. Ecological Applications 22:1246–1256.

Klein, C. J., S. D. Jupiter, M. Watts, and H. P. Possingham. 2014. Evaluating the influence of candidate terrestrial protected areas on coral reef condition in Fiji. Marine Policy 44:360–365.

Knowlton, N., and J. B. Jackson. 2008. Shifting baselines, local impacts, and global change on coral reefs. PLoS biology 6: e54.

Knudby, A., C. Roelfsema, M. Lyons, S. Phinn, and S. Jupiter. 2011. Mapping fish community variables by integrating field and satellite data, object-based image analysis and modeling in a traditional Fijian fisheries management area. Remote Sensing 3:460–483.

Kueffer, C., and K. Kinney. 2017. What is the importance of islands to environmental conservation? Environmental Conservation 44:311–322.

Lianes, E., M. Marchamalo, and M. Roldán. 2009. Evaluación del factor C de la RUSLE para el manejo de coberturas vegetales en el control de la erosión en la cuenca del río Birrís, Costa Rica. Agronomía Costarricense 33:217–235.

López-Vicente, M., J. Poesen, A. Navas, and L. Gaspar. 2013. Predicting runoff and sediment connectivity and soil erosion by water for different land use scenarios in the Spanish Pre-Pyrenees. Catena 102:62–73.

Margules, C. R., and R. L. Pressey. 2000. Systematic conservation planning. Nature 405:243–253.

Mather, A. S., C. L. Needle, and J. Fairbairn. 1998. The human drivers of global land cover change: the case of forests. Hydrological processes 12:1983–1994.

McIntosh, P. D. 2013. Review of soil and water provisions in the Papua New Guinea Logging Code of Practice and related codes in the tropics, A report under Project GCP. PNG/003/AUL for the PNG Forest Authority, the Food and Agriculture Organisation of the United Nations and the Australian Government Department of Agriculture, Fisheries and Forestry.

Morgan, K. M., C. T. Perry, J. A. Johnson, and S. G. Smithers. 2016. Nearshore Turbid-Zone Corals Exhibit High Bleaching Tolerance on the Great Barrier Reef Following the. Page 224.

Morrison, R. J., W. C. Clarke, N. V. Buresova, and L. Limalevu. 1990. Erosion and sedimentation in Fiji-an overview. Erosion and sedimentation in Fiji-an overview.:14–23.

Mumby, P. J. 2017. Embracing a world of subtlety and nuance on coral reefs. Coral Reefs 36:1003–1011.

Olley, J., J. Burton, V. Hermoso, K. Smolders, J. McMahon, B. Thomson, and A. Watkinson. 2015. Remnant riparian vegetation, sediment and nutrient loads, and river rehabilitation in subtropical Australia. Hydrological Processes 29:2290–2300.

OMAFRA. 2019. Universal Soil Loss Equation (USLE). http://www.omafra.gov.on.ca/english/engineer/facts/12-051.htm.

Pierce, D. 2019. ncdf4: Interface to Unidata netCDF (Version 4 or Earlier).

Regenvanu, R., S. W. Wyatt, and L. Tacconi. 1997. Changing forestry regimes in Vanuatu: is sustainable management possible? The Contemporary Pacific:73–96.

Reichert, P., and M. E. Borsuk. 2005. Does high forecast uncertainty preclude effective decision support? Environmental Modelling & Software 20:991–1001.

Renard, K. G., G. R. Foster, G. A. Weesies, D. K. McCool, and D. C. Yoder. 1997. Predicting soil erosion by water: a guide to conservation planning with the Revised Universal Soil Loss Equation (RUSLE). United States Department of Agriculture Washington, DC.

Roelfsema, C., S. Phinn, S. Jupiter, J. Comley, and S. Albert. 2013. Mapping coral reefs at reef to reef-system scales, 10s–1000s km2, using object-based image analysis. International journal of remote sensing 34:6367–6388.

Rogers, C. S. 1990. Responses of coral reefs and reef organisms to sedimentation. Marine ecology progress series. Oldendorf 62:185–202.

Roose, E. J. 1977. Use of the universal soil loss equation to predict erosion in West Africa. Pages 60–74 Soil erosion: prediction and control. Soil Conservation Society of America Ankeny, IA.

Rude, J., A. Minks, B. Doheny, M. Tyner, K. Maher, C. Huffard, N. I. Hidayat, and H. Grantham. 2016. Ridge to reef modelling for use within land–sea planning under data-limited conditions. Aquatic Conservation: Marine and Freshwater Ecosystems 26:251–264.

Saunders, M. I., S. Atkinson, C. J. Klein, T. Weber, and H. P. Possingham. 2017. Increased sediment loads cause non-linear decreases in seagrass suitable habitat extent. PloS One 12:e0187284.

Sharp, R., H. T. Tallis, T. Ricketts, A. D. Guerry, S. A. Wood, R. Chaplin-Kramer, E. Nelson, D. Ennaanay, S. Wolny, and N. Olwero. 2016. InVEST+ VERSION+ User's Guide. The Natural Capital Project. Stanford University, University of Minnesota, The Nature Conservancy, and World Wildlife Fund.

Smith, J. E., R. Brainard, A. Carter, S. Grillo, C. Edwards, J. Harris, L. Lewis, D. Obura, F. Rohwer, E. Sala, P. S. Vroom, and S. Sandin. 2016b. Re-evaluating the health of coral reef communities: baselines and evidence for human impacts across the central Pacific. Proc. R. Soc. B 283:20151985.

Szmant, A. M. 2002. Nutrient enrichment on coral reefs: Is it a major cause of coral reef decline? Estuaries, 25(4): 743 – 766.

Team, Q. D. 2015. QGIS geographic information system. Open Source Geospatial Foundation Project, Versão 2.

Team, R. C. 2014. R: A language and environment for statistical computing. R Foundation for Statistical Computing.

Toonen, R. J., K. R. Andrews, I. B. Baums, C. E. Bird, G. T. Concepcion, T. S. Daly-Engel, J. A. Eble, A. Faucci, M. R. Gaither, M. Iacchei, J. B. Puritz, J. K. Schultz, D. J. Skillings, M. A. Timmers, and B. W. Bowen. 2011. Defining Boundaries for Ecosystem-Based Management: A Multispecies Case Study of Marine Connectivity across the Hawaiian Archipelago. Journal of Marine Biology 2011:13.

Tulloch, V. J., C. J. Brown, H. P. Possingham, S. D. Jupiter, J. M. Maina, and C. Klein. 2016. Improving conservation outcomes for coral reefs affected by future oil palm development in Papua New Guinea. Biol Conserv 203:43–54.

Walker, L. R., and P. Bellingham. 2011. Island Environments in a Changing World. Cambridge University Press.

Weatherall, P., K. M. Marks, M. Jakobsson, T. Schmitt, S. Tani, J. E. Arndt, M. Rovere, D. Chayes, V. Ferrini, and R. Wigley. 2015. A new digital bathymetric model of the world's oceans. Earth and Space Science 2:331–345.

Weijerman, M., L. Veazey, S. Yee, K. Vaché, J. Delevaux, M. Donovan, J. Lecky, and K. L. Oleson. 2018. Managing local stressors for coral reef condition and ecosystem services delivery under climate scenarios. Frontiers in Marine Science 5:425.

Wenger, A. S., M. I. McCormick, G. G. Endo, I. M. McLeod, F. J. Kroon, and G. P. Jones. 2014. Suspended sediment prolongs larval development in a coral reef fish. Journal of Experimental Biology 217:1122–1128.

Wenger, A. S., D. H. Williamson, and T. E. Da. 2015. Effects of reduced water quality on coral reefs in and out of no-take marine reserves. Conservation Biology 30:142–153.

Williams, J. R. 1995. The EPIC model. Computer models of watershed hydrology:909–1000.

Wilson, S. K., R. Fisher, M. S. Pratchett, N. a. J. Graham, N. K. Dulvy, R. A. Turner, A. Cakacaka, and and N. V. C. Polunin. 2010. Habitat degradation and fishing effects on the size structure of coral reef fish communities. Ecological Applications 20:442–451.

Wischmeier, W. H., and D. D. Smith. 1978. Predicting rainfall erosion losses: a guide to conservation planning. Science and Education Administration, US Department of Agriculture.

Wooldridge, S. A. 2009. Water quality and coral bleaching thresholds: Formalising the linkage for the inshore reefs of the Great Barrier Reef, Australia. Marine Pollution Bulletin 58:745–751.

Wooldridge, S. A., and Done. 2009. Improved water quality can ameliorate effects of climate change on corals. Ecological Applications 19:1492–1499.

Yentsch, C. S., C. M. Yentsch, J. J. Cullen, B. Lapointe, D. A. Phinney, and S. W. Yentsch. 2002. Sunlight and water transparency: cornerstones in coral research. Journal of Experimental Marine Biology and Ecology 268:171–183.

Yu, C., J. A. Y. Lee, and M. J. Munro-Stasiuk. 2003. Extensions to least-cost path algorithms for roadway planning. Int J Geogr Inf 17:361–376.

7. APPENDIX

Table S1. Present land cover type, area (km^2), and percent cover

Land cover / Land use	Area (km2)	%
Airstrip	0.03	0.00
Banana	0.07	0.00
Barren Land	0.09	0.00
Cassava/yams	0.13	0.00
Coconut Crops/plantation	550.01	4.53
Coconut Forest	161.91	1.33
Cultivated Land	0.48	0.00
Forest	9980.47	82.29
Legumes	0.01	0.00
Limestone	0.00	0.00
Navel Nut/Noni Tree	0.90	0.01
Open Land	1241.00	10.23
Pine Plantation	11.83	0.10
Plantation	75.36	0.62
Rice	3.39	0.03
Rock Shelves	0.04	0.00
Sand Bay	1.68	0.01
Settlement	32.59	0.27
Shrubs	4.15	0.03
Sugarcane	0.12	0.00
Volcanic Ash Plain	64.33	0.53
Total	12128.6	100

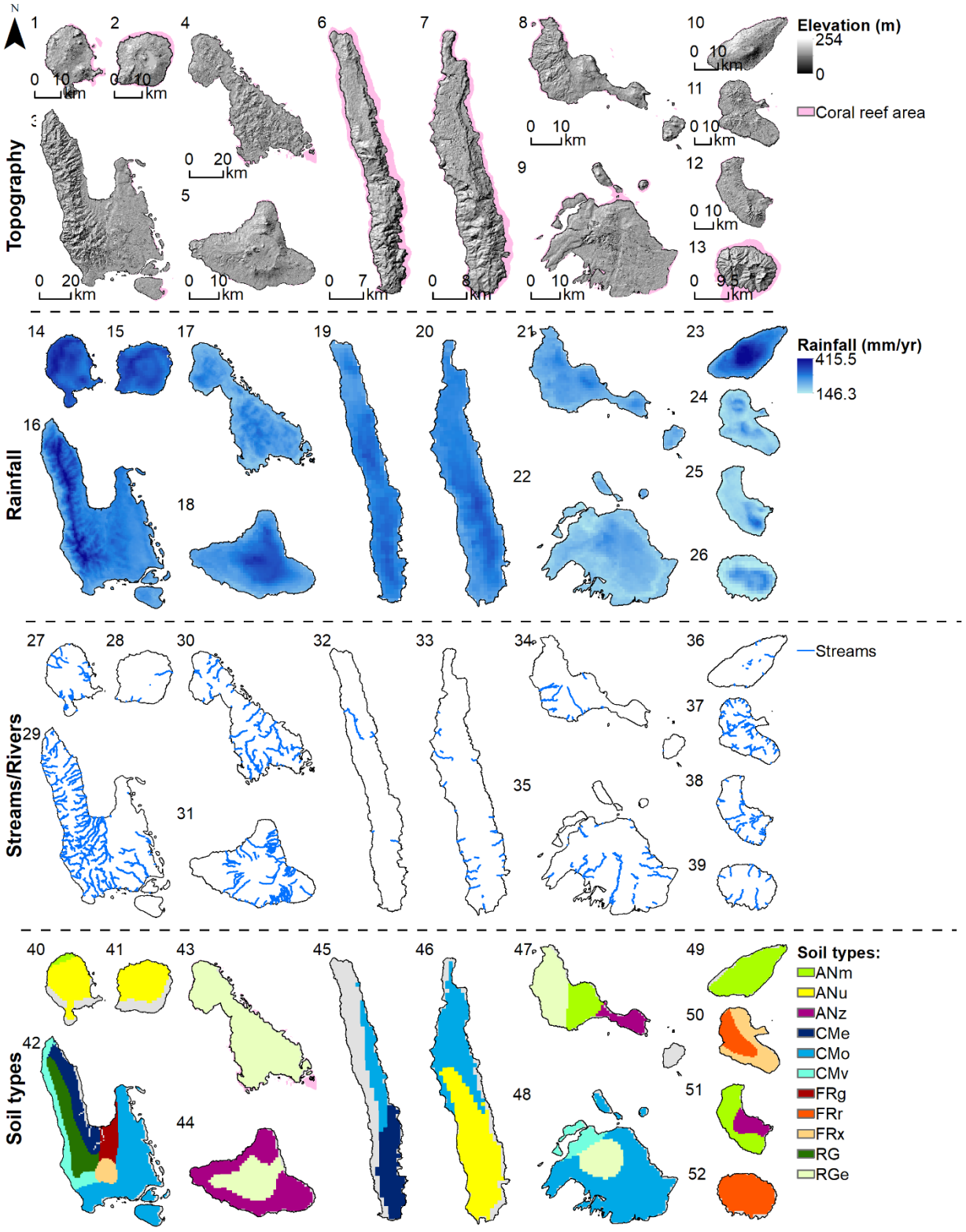

Fig S1. Terrestrial geography

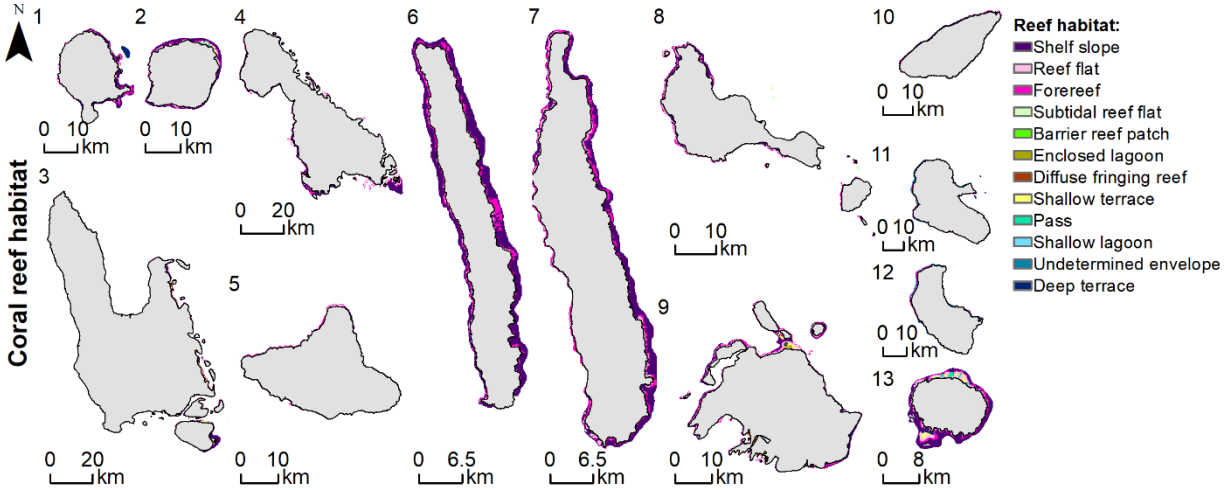

Fig. S2. Coral reef key habitats

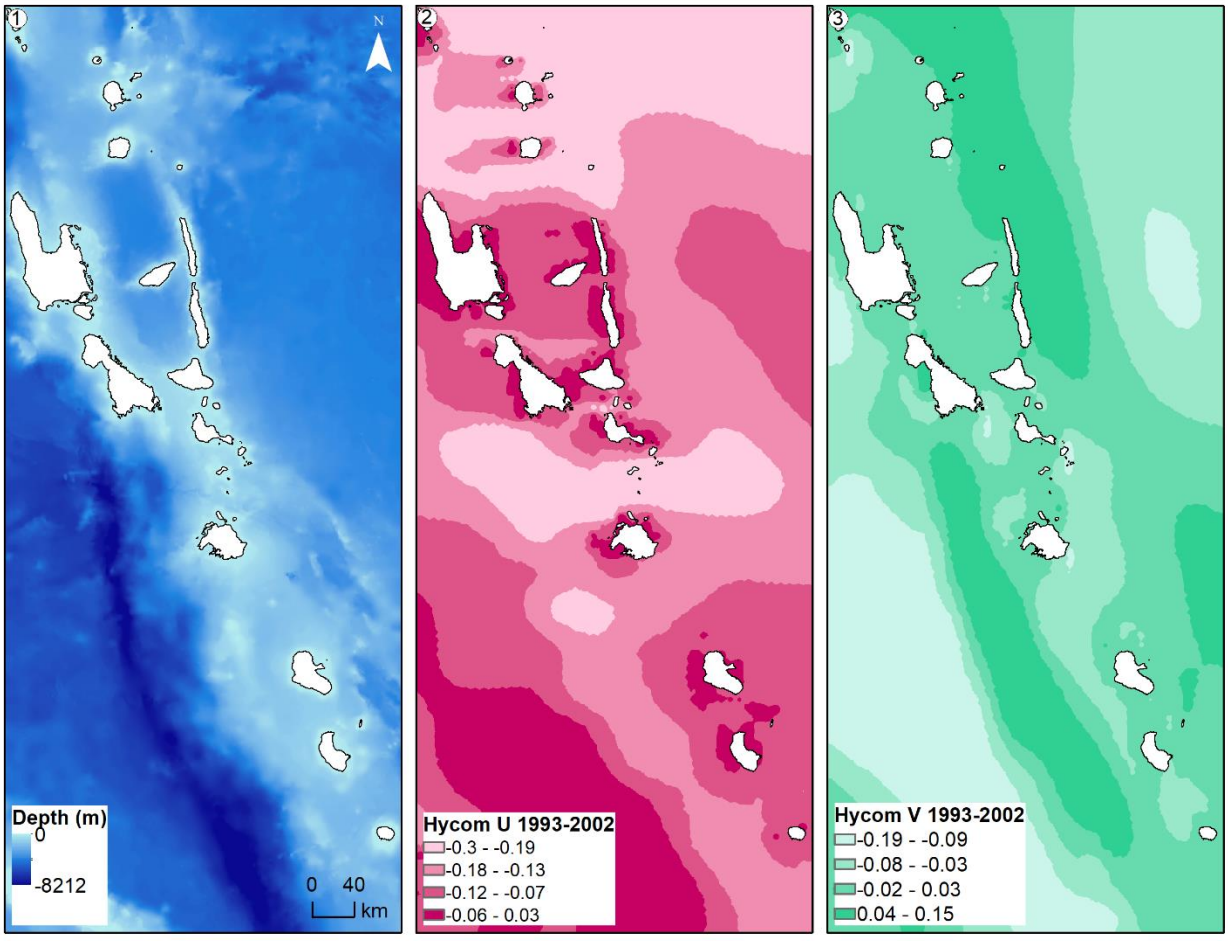

Fig S3. Marine geography

Text S1. Key assumptions & modeling caveats (adapted from Delevaux et al. 2018)

Modeling requires simplifying the reality and making assumptions. The first key simplification is the static nature of this modeling approach. Although, our sediment models accounted for the connectivity across the landscape (Hamel et al. 2015), this tool relies on static modeling and does not explicitly model the response of coral reef indicators to TSS change, meaning, our framework is not set up to provide information on degradation or recovery trajectories of impacted ecosystems (Gurney et al. 2013, Weijerman et al. 2018). Instead, we undertook an overlay analysis, where we assumed a potential adverse impact where significant changes in TSS occurred over a coral reef habitat. Empirical research has shown that coral reefs chronically exposed to high turbidity can be less vulnerable to sediment impacts (Anthony 2006, Morgan et al. 2016). In that case, it is possible that we overestimated the impact of increased TSS on the reefs located near the source of the sediment plume and underestimated the impact offshore. Research has highlighted that coral reefs are spatially heterogeneous and nuanced ecosystems (Mumby 2017). For instance, certain habitat categories could host coral cover in shallow waters but likely not in depths beyond 25 m. Because the bathymetry layer is coarse resolution and interpolated in the nearshore, we were not able to reliably define an offshore modeling boundary based on depth beyond which we could assume no impact on reefs. Instead we limited our impact assessment to the reef habitat map.

Another key assumption associated with predicting futures with static models is that the effects of time lags and the complex, nonlinear relationships between land-use practices and coral reef benefits are not accounted for, which can influence management scale and outcomes (Toonen et al. 2011). For instance, the deforestation scenarios assumed all clearing was immediate. In reality, clearing proceeds in a patchwork over time and different areas would have different amounts of ground cover or regrowth at different times (Tulloch et al. 2016), therefore sediment export would differ from the total export modeled here. From a marine perspective, coral reef response to change in sediment runoff will also vary over time based on taxon physiology and environmental conditions (Anthony 2006). Thus, from a management perspective, it is essential to account for the timeframe of anticipated outcomes of conservation actions to factor in social and economic constraints (Saunders et al. 2017). Our findings indicate that forest conservation actions on land should be a high priority because they can also promote coral reef resilience. However, we only explicitly considered land-use change in terms of local actions in our scenarios and did not evaluate the potential benefits from marine-based conservation actions.

Uncertainty is inherent in modeling complex systems (Reichert and Borsuk 2005) and arises at all stages of the modeling process (Gurney et al. 2013). Given imperfect knowledge of all the land-sea processes on coral reefs, scenario modeling requires simplifications and assumptions which lead to uncertainty in model projections (Delevaux et al. 2018). Although we used present conditions as the baseline for examining projected coral reefs, this comparative benchmark represents potentially impacted ecosystems (Knowlton and Jackson 2008). However, present conditions still provide an opportunity to identify the trajectory of coral reefs under different human drivers and provide guidance for management (Alagona et al. 2012). Given that sources of uncertainty in scenario analysis are inevitable, we used scenario modeling to illustrate the range

of possibilities for the future of these islands. This approach spatially identified the drivers of water quality degradation while also providing guidance on priority locations where local management could be most effective. Additionally, these findings can help achieve more effective management outcomes by indicating where coral reefs and associated marine resources may be at higher risk (Coreau et al. 2009, Gurney et al. 2013).